Plasma-derived extracellular vesicles released after endurance exercise exert cardioprotective activity through the activation of antioxidant pathways

Lisi, Veronica ; Senesi, Giorgia ; Bertola, Nadia ; Pecoraro, Matteo ; Bolis, Sara ; Gualerzi, Alice ; Picciolini, Silvia ; Raimondi, Andrea ; Fantini, Cristina ; Moretti, Elisa ; Parisi, Attilio ; Sgrò, Paolo ; Di Luigi, Luigi ; Geiger, Roger ; Ravera, Silvia ; Vassalli, Giuseppe ; Caporossi, Daniela ; Balbi, Carolina

DOI: https://doi.org/10.1016/j.redox.2023.102737

Redox Biology 63 (2023) 102737

Contents lists available at ScienceDirect

Redox Biology

journal homepage: www.elsevier.com/locate/redox

Plasma-derived extracellular vesicles released after endurance exercise exert cardioprotective activity through the activation of antioxidant pathways

Veronica Lisi [a], Giorgia Senesi [b,c], Nadia Bertola [d], Matteo Pecoraro [e], Sara Bolis [f], Alice Gualerzi [g], Silvia Picciolini [g], Andrea Raimondi [e,h], Cristina Fantini [a], Elisa Moretti [i], Attilio Parisi [i], Paolo Sgrò [i], Luigi Di Luigi [j], Roger Geiger [e], Silvia Ravera [d], Giuseppe Vassalli [b,c,k], Daniela Caporossi [a,1], Carolina Balbi [b,k,*,1]

[a] Unit of Biology and Genetics of Movement, Department of Movement, Human and Health Sciences, University of Rome Foro Italico, Piazza Lauro de Bosis 15, 00135, Rome, Italy
[b] Cellular and Molecular Cardiology, Istituto Cardiocentro Ticino, Laboratories for Translational Research, Ente Ospedaliero Cantonale, Bellinzona, Switzerland
[c] Faculty of Biomedical Sciences, Università della Svizzera Italiana, Lugano, Switzerland
[d] Department of Experimental Medicine, University of Genoa, 16132, Genova, Italy
[e] Institute for Research in Biomedicine, Università della Svizzera italiana, Bellinzona, Switzerland
[f] Cardiovascular Theranostics, Istituto Cardiocentro Ticino, Laboratories for Translational Research, Ente Ospedaliero Cantonale, Bellinzona, Switzerland
[g] Laboratory of Nanomedicine and Clinical Biophotonics (LABION), IRCCS Fondazione Don Carlo Gnocchi, Milan, Italy
[h] Centro Imaging Sperimentale, IRCCS Istituto Scientifico San Raffaele, Via Olgettina 52, 20132, Milan, Italy
[i] Laboratory of Physical Exercise and Sport Science, Department of Exercise, Human and Health Sciences, University of Rome Foro Italico, Piazza Lauro de Bosis 15, 00135, Rome, Italy
[j] Endocrinology Unit, Department of Movement, Human and Health Sciences, University of Rome Foro Italico, Piazza Lauro de Bosis 15, 00135, Rome, Italy
[k] Center for Molecular Cardiology, Zurich, Switzerland

ARTICLE INFO

Keywords:
Physical exercise
Extracellular vesicles
Cardioprotection
Redox capacity
Antioxidant activity
Catalytic activity

ABSTRACT

Cardiovascular diseases (CVD) can cause various conditions, including an increase in reactive oxygen species (ROS) levels that can decrease nitric oxide (NO) availability and promote vasoconstriction, leading to arterial hypertension. Physical exercise (PE) has been found to be protective against CVD by helping to maintain redox homeostasis through a decrease in ROS levels, achieved by increased expression of antioxidant enzymes (AOEs) and modulation of heat shock proteins (HSPs). Extracellular vesicles (EVs) circulating in the body are a major source of regulatory signals, including proteins and nucleic acids. Interestingly, the cardioprotective role of EVs released after PE has not been fully described.

The aim of this study was to investigate the role of circulating EVs, obtained through Size Exclusion Chromatography (SEC) of plasma samples from healthy young males (age: 26.95 ± 3.07; estimated maximum oxygen consumption rate (VO_{2max}): 51.22 ± 4.85 (mL/kg/min)) at basal level (Pre_EVs) and immediately after a single bout of endurance exercise (30' treadmill, 70% heart rate (HR) -Post_EVs). Gene ontology (GO) analysis of proteomic data from isolated EVs, revealed enrichment in proteins endowed with catalytic activity in Post_EVs, compare to Pre_EVs, with MAP2K1 being the most significantly upregulated protein. Enzymatic assays on EVs derived from Pre and Post samples showed increment in Glutathione Reductase (GR) and Catalase (CAT) activity in Post_EVs. At functional level, Post_EVs, but not Pre_EVs, enhanced the activity of antioxidant enzymes (AOEs) and reduced oxidative damage accumulation in treated human iPS-derived cardiomyocytes (hCM) at basal level and under stress conditions (Hydrogen Peroxide (H_2O_2) treatment), resulting in a global cardioprotective effect.

In conclusion, our data demonstrated, for the first time, that a single 30-min endurance exercise is able to alter the cargo of circulating EVs, resulting in cardioprotective effect through antioxidant activity.

* Corresponding author. Cellular and Molecular Cardiology, Istituto Cardiocentro Ticino, Laboratories for Translational Research, Ente Ospedaliero Cantonale, Bellinzona, Switzerland.
E-mail address: carolina.balbi@eoc.ch (C. Balbi).
[1] These authors equally contributed to the study.

https://doi.org/10.1016/j.redox.2023.102737
Received 22 March 2023; Received in revised form 8 May 2023; Accepted 8 May 2023
Available online 18 May 2023

Abbreviations

H_2O_2	Hydrogen Peroxide
PE	Physical exercise
CVD	Cardiovascular disease
ROS	Reactive oxygen species
NO	Nitric oxide
PBMCs	Peripheral blood mononuclear cell
NRF2	Nuclear factor erythroid 2-related factor 2
AOEs	antioxidant enzymes
CAT	Catalase
SOD1	Superoxide dismutase 1
HMOX1	Heme Oxygenase 1
NQO1	NAD(P)H quinone dehydrogenase 1
EVs	Extracellular Vesicles
VO_{2max}	Maximal oxygen consumption
HR	Heart rate
SEC	Size exclusion chromatography
NTA	Nanoparticle tracking analysis
SPRi	Surface Plasmon Resonance imaging
hCM	human-induced cardiomyocyte
TBARS	Thiobarbituric acid reactive substances
GR	Glutathione Reductase
GPx	Glutathione Peroxidase
G6PD	Glucose-6-Phosphate Dehydrogenase
DCF	2',7'-dichlorofluorescein
DHE	Dihydroethidium
E^+	ethidium
2-OH-E^+	2-hydroxyethidium
O_2^-	Superoxide
MAP2K1	mitogen-activated protein kinase kinase 1
CNDP2	Carnosine dipeptidase 2
GCLM	Glutamate-cysteine ligase modifier subunit
MGST2	Microsomal glutathione S-transferase 2
HSPs	Heat shock proteins
GO	Gene Ontology
MVs	Microvesicles
MVBs	Multi vesicular bodies
RBCs	Red blood cells

1. Introduction

1.1. Physical exercise and redox homeostasis

Physical exercise (PE) has numerous benefits for the cardiovascular system [1]. Exercise improves heart function, blood circulation, and blood pressure while promoting healthy weight maintenance [2,3]. As a result, PE is a powerful tool for promoting heart health and reducing the risk of cardiovascular disease (CVD) [4]. Interestingly, the imbalance between pro-oxidant and antioxidant factors is a major contributor to the onset and progression of various diseases, including CVD [5]. Increase in reactive oxygen species (ROS) can lead to decrement in nitric oxide (NO) availability with consequent vasoconstriction and promotion of arterial hypertension [6]. However, even if oxidative stress is an imbalance between ROS production and/or a decrease in antioxidants, better to distinguish between two types of oxidative stress: "oxidative distress" and "oxidative eustress". The first one leads to molecular damage, while the second shows central role in redox signalling via different post-translational modifications [7]. Muscle and other cell types (e.g., peripheral blood mononuclear cell-PBMCs) can increase ROS production in response to an acute exercise [8]. On the other hand, a transient regular exercise can trigger oxidative eustress which can help maintain redox homeostasis by the activation of trascriptional factors, such as nuclear factor erythroid 2-related factor 2 (NRF2) [9]. NRF2 nuclear translocation can regulated the expression of antioxidant enzymes (AOEs) such as Catalase (CAT), Superoxide dismutase 1 (SOD1), heme oxygenase-1 (HMOX1), and NAD(P)H quinone dehydrogenase 1 (NQO1) [10–14]. Indeed, it has been demonstrated that regular physical exercise in healthy people leads to a systemic adaptation to redox homeostasis perturbation, one of the hallmarks of exercise adaptation [15,16]. Exercise-induced inter-tissue communication is thought to have a major role on this adaptation. Specifically, PE induces release of peptides and nucleic acids from skeletal muscle and other organs, known as "exerkines", which play a crucial role in mediating systemic adaptations, promoting the crosstalk between organs and potentiating the systemic benefits of exercise [17–19]. However, not all molecules can be released with a canonical secretion-targeting sequence, or with a stimulus-dependent pathway. Interestingly, peptides, metabolites, DNA, mRNA, miRNA, and other RNA species can be transport by extracellular vesicles (EVs) [20,21].

1.2. Physical exercise and extracellular vesicles

EVs are small, membrane-bound structures that are released from cells into the bloodstream and play a role in cell-to-cell communication [22] by transporting and delivering bioactive molecules such as proteins and RNA that contribute to intracellular signalling pathways and regulate functions in recipient cells [23,24]. Studies have shown that PE can alter the molecular composition of EVs, impacting their ability to communicate with other cells and modulate physiological processes [25]. Circulating EVs play a pivotal role in the cardiovascular system, regulating diverse functions in target cells, maintaining cardiovascular balance and health, or inducing pathological changes in CVD [26]. Indeed, miRNAs and proteins transferred by EVs play essential roles in maintaining normal cardiac structure and function under physiological conditions [27]. On the other hand, it is known that EVs change the composition of their cargo under different conditions, such as pathological ones, which gives rise to the development of CVD [28]. Interestingly, even PE can modulate extracellular vesicle release and their cargo [29,30]. Different physiological stimuli during PE led to an alteration of the EVs landscape in blood. Analysis of the protein cargo of EVs obtained after PE identified various proteins associated with key signalling pathways, including angiogenesis, immune signalling, and glycolysis [31]. Additionally, several studies evidenced an altered miRNAs panel in EVs in response to exercise bouts or training [29,32,33]. Some of the miRNAs carried by circulating EVs obtained post-PE belong to the group of myomiRs, indicating the involvement of EVs in muscle regeneration processes following exercise [34]. Functional analysis of these vesicles suggests contribution to cardioprotection in ischemia/reperfusion injury [35], endothelial function [36], as well as muscle remodelling and growth [37].

In this study, we hypothesize that PE, understood as a single short-term acute endurance exercise, can modulate the cargo of circulating EVs, resulting in an increase in antioxidant proteins that have cardioprotective functions.

2. Material and methods

2.1. Subjects' characteristics

A total of 21 healthy male subjects, matched for the age and body mass index (26.95 ± 3.07 years, body mass index: 23.51 ± 2.25), with an active lifestyle, corresponding to a medium/high fitness level (40.98

< VO_{2max} < 58.31 mL/kg/min obtained indirectly through the Balke's Test) [38], have been recruited for this study at the University of Rome "Foro Italico" (Supplementary Fig. 1). All the participants were subjects to Baecke Questionnaire developed for evaluating a person's physical activity [39]. The questionnaire is divided into three different areas: the Work Index concerning the physical activity during working hours (sedentary, active or heavy); the Sports Index reporting the type of sports practiced, and the Leisure Index concerning physical activity during leisure time activities. The scores of the three indexes are summed to obtain the questionnaire's total score. The lower the score on the questionnaire, the higher the level of physical activity performed. All subjects underwent a detailed medical history and physical examination and provided informed written consent approved by the University of Rome Ethics Committee "Sapienza" (RIF.CE: 4521). Moreover, each participant completed a detailed eating habits diary in which they recorded food and drinks consumed during the 3 consecutive days before the beginning of the exercise protocol. None of them was an elite athlete neither reported any illness or ongoing medication. Exclusion criteria: signs of cardiovascular, metabolic, and pulmonary disease; orthopaedic injury or joint disease; and neurological or immunologic disease.

2.2. Physical fitness level and endurance exercise protocol

Before starting the acute endurance exercise protocol, each participant performed the Balke Treadmill Test, an incremental test aimed to estimate indirectly the VO_{2max}. This continuous incremental test, performed on a treadmill (Skillrun Treadmill, Technogym), assesses the aerobic capacity of participants. The test began with a warm-up of 5 min at 5.3 km/h with a slope of 0°; then the operator increased the slope by 1° each minute until the 18th minute, after that the speed was increased by 0.3 km/h per minute, simultaneously to each increment the HR was measured via heart rate monitor chest strap (Polar M400) and fatigue was assessed with the Borg Scale 0–20 [40]. The test was completed when the participant could no longer walk or run at the slope and speed reached. The score is estimated using the test time (T - time spent walking on the treadmill till exhaustion, in minutes) in the following formula [VO_{2max} = 1.444 (T) + 14.99]. Average time spent on the treadmill was between 9 and 15 min. To indirectly target the aerobic threshold during the test, the 70% of Heart Rate (HR) was estimated using the Karvonen formula ((220- age of participant) - HR]*70% + HR at rest). To identify the correct slope and speed required to reach 70% of the maximum HR, HR was monitored during the Balke test. These parameters were used to target the aerobic training protocol using the right workout intensity. The mean value of participant's 70% HR was 154bpm 7,50 SD.

2.3. Blood sampling

Before (Pre) and immediately after (Post) endurance exercise (30' treadmill, 70% HR) protocol, blood samples were drawn from the antecubital vein from the volunteers (Supplementary Fig. 1). Plasma was obtained from whole blood samples collected in EDTA tubes and centrifugated, 20 min after the sampling, at 1200 g × 10 min, then divided into 500 μl aliquots and stored at −80C° for further analysis.

2.4. Extracellular vesicles isolation

Plasma EVs were isolated using Size Exclusion Chromatography (SEC). SEC was performed using commercially available columns according to the manufacturer's instructions (q70nm column-Izon). Briefly, 500 μl of plasma was centrifuged at 3000 g for 15 min to remove cells' debris. The supernatant was added to the top of the column and then eluted using PBS1X. Fractions 7-8-9-10 enriched in EVs were collected and used for further experiments.

2.5. EV characterization: Nanoparticle Tracking Analysis

Nanoparticle Tracking analysis (NTA) measurement was carried out with Zetaview (Particle Metrix). Shortly, 1 μl of plasma samples, or EVs isolated from plasma, were diluted in PBS1X to a final volume of 1 ml. The manufacturer's default software settings for EVs or nanospheres were selected accordingly. For each measurement, 11 cell positions with a cell temperature of 25°C were acquired. After capture, videos were analysed by the in-build ZetaView Software 8.02.31. Hardware: embedded laser: 40 mW at 520 nm; camera: CMOS. The number of completed tracks in NTA measurements was always greater than the proposed minimum of 1,000 in order to minimize data skewing based on single large particles. Particle number was expressed in number/ml and size (diameter) in nm.

2.6. EV characterization: Western blot

Total proteins were extracted from isolated EVs by lysing samples with ice-cold RIPA buffer supplemented with SIGMAFAST™ Protease Inhibitors and Phosphatase Inhibitor Cocktail 3 and 2 (all from Sigma). Proteins were boiled with Laemmli SDS sample buffer 6X (VWR International), separated on 4–20% MiniPROTEAN®TGX™ Precast Gel, and transferred onto a PVDF membrane with a semi-dry transfer system (all from Bio-Rad Europe, Basel, Switzerland). Membranes were incubated with ALIX (Abcam ab186429; 1:1000), TSG101 (Abcam ab125011, 1:1000), and Syntenin-1 (Abcam ab19903; 1:1000) and Apolipoprotein A1 (APOA1) (Invitrogen 701239, 1:500) primary antibodies. Secondary antibodies IRDye® 680RD or 800CW goat anti-mouse or goat anti-rabbit (LI-COR Biosciences) were used for detection. The infrared signal was detected using Odyssey CLx Detection System (LI-COR Biosciences).

2.7. EV characterization: Transmission Electron Microscopy (TEM) analysis

Morphological evaluations of isolated Pre and Post derived-EVs were performed using Transmission Electron Microscopy (TEM) negative staining. EVs derived from 200 μl of plasma were diluted 1:100 and absorbed on a glow-discharged carbon-coated formvar copper grid and negatively stained with 2% uranyl acetate. EVs pictures were examined by a Talos L120C (FEI, Thermo Fisher Scientific) operating at 120 kV. Images were acquired with a Ceta CCD camera (FEI, Thermo Fisher Scientific).

2.8. EV characterization: Surface plasmon resonance imaging (SPRi) analysis

In SPRi biochip preparation and experiments, all reagents were purchased from Merck KGaA (Darmstadt) and used without any further purification, if not stated otherwise. To detect different subfamilies of EVs circulating in plasma, the SPRi biosensor was prepared following a previously optimized procedure [41,42]. Briefly, prior to the ligand conjugation, the chip surface was cleaned with piranha solution and rinsed with ultrapure water and ethanol. Then, the SPRi gold chips were coated with a Self-Assembled Monolayer (SAM) of thiolated PEG molecules (TH 001-m11.n2 and TH 003-m11.n6; ProChimia Surfaces) for the conjugation of ligands on the chip, using EDC/NHS chemistry. An array of antibodies/lectin was conjugated on top of the chip using the automated spotter iFOUR Dispensing System (M24You) thanks to a Piezo Driven Micro-Dispenser (PDMD) equipped with a 130 mm long borosilicate glass capillary and a cylindrical piezo ceramic actuator. The families of ligands spotted on a chip for the microarray preparation are the following: anti-CD36 (33621, Biolegend), anti-CD31 (11-0311-82, Invitrogen), anti-CD106 (MA5-16429, Invitrogen), isolectin B4 (IB4) from Bandeiraea simplicifolia (L3019, Merck), anti-CD11b (553311, BD Biosciences, San Jose, CA, USA), Anti-Irisin (MAB9420-100, Bio-Techne). An anti-rat IgG1 antibody (407402, BioLegend Inc, San Diego,

CA, USA) was used as a negative control. After ligand immobilization, the chip was blocked in a solution of ethanolamine (1 M; pH 9) for 30 min, washed with water, and stored at 4 °C until use.

2.9. SPRi measurements

The XelPleX instrument (Horiba Scientific SAS) was used for the simultaneous detection of multiple subfamilies of EVs. After accurate instrument calibration (200 µl of sucrose 3 mg/ml at 50 µl/min flow rate), experiments were performed using PBS1X as the running buffer. For each sample, the same amount of proteins calculated by BCA assay (40 µg/ml) was injected in the SPRi flow chamber with a flow rate of 25 µl/min. Detection of the interactions between EVs and each ligand was performed in real-time through the analysis of SPRi signal intensity at the end of the association phase. This analysis provided quantitative information on the relative amount of EVs coming from distinct cells in the plasma. Data analysis was performed using EzSuite (Horiba) and Origin2021 (OriginLab) software. The signal obtained on antibody anti-IgG spots was subtracted from the signals obtained on all the other ligands present on the same chip.

2.10. Proteomic analysis: protein extraction and enzymatic digestion

EVs lysis and protein extraction were performed in 4% sodium dodecyl sulfate (SDS) in 100 mM Tris pH 7.6 by sonication in a Bioruptor (Diagenode, 15 cycles, 30s on, 30s off, high mode) and incubation at 95°C for 10 min. Proteins were then precipitated overnight in 80% cold acetone. The next day, proteins were pelleted by centrifugation at 13000 rpm for 20 min at 4°C, washed with 80% cold acetone, and dried at 40°C. The pellets were then resuspended in 8 M urea in 50 mM ammonium bicarbonate (ABC) through another sonication in a Bioruptor (same settings). Proteins were reduced with 10 mM dithiothreitol for 20 min at room temperature and alkylated with 50 mM iodoacetamide for 30 min at room temperature. Protein digestion was performed with LysC (Wako Fujifilm, 1:100 w/w) for 2 h at room temperature, after which the digestion buffer was diluted to 2 M urea with 50 mM ABC and trypsin (Promega, 1:100 w/w) was added for overnight digestion at room temperature. Digestion was stopped by adding acetonitrile (ACN) to 2% and trifluoroacetic acid (TFA) to 0.3% and the samples were cleared by centrifugation for 5 min at maximum speed. The resulting peptides were purified on C18 StageTips [43], and eluted with 80% ACN and 0.5% acetic acid. Finally, the elution buffer was evaporated by vacuum centrifugation, and the purified peptides were resuspended in 2% ACN, 0.5% acetic acid, and 0.1% TFA for single-shot LC-MS/MS measurements.

2.11. LC-MS/MS analysis

Peptides were separated on an EASY-nLC 1200 HPLC system (Thermo Fisher Scientific) coupled online via a nanoelectrospray source (Thermo Fisher Scientific) to a Q Exactive HF mass spectrometer (Thermo Fisher Scientific). Peptides were loaded in buffer A (0.1% formic acid) on a 75 µm inner diameter, 50 cm length column in-house packed with ReproSil-Pur C18-AQ 1.9 µm resin (Dr. Maisch HPLC GmbH) and eluted over a 150-min linear gradient of 5 to 30% buffer B (80% ACN, 0.1% formic acid) with a 250 nl/min flow rate. The Q Exactive HF was operated in a data-dependent mode through the Xcalibur software (Thermo Scientific), with a MS scan range of 300-1,650 *m/z*, resolution of 60,000 at 200 *m/z*, maximum injection time of 20 ms, and AGC target of 3e6. The 10 most abundant ions with charge 2 to 5 were isolated with a 1.8 *m/z* isolation window and fragmented by higher-energy collisional dissociation (HCD) at a normalized collision energy of 27. MS/MS spectra were acquired with a resolution of 15,000 at 200 *m/z*, a maximum injection time of 55 ms, and an AGC target of 1e5. Dynamic exclusion was set to 30 s to reduce repeated sequencing.

2.12. LC-MS/MS data analysis

MS raw files were processed using the MaxQuant software v.1.6.7.0 (Cox & Mann, 2008). The integrated Andromeda search engine [44] was employed to search spectra against the Human UniProt database (June 2019) and a common contaminants database (247 entries) to identify peptides and proteins with a false discovery rate of <1%. Enzyme specificity was set to "Trypsin/P" with a maximum of 2 missed cleavages and a minimum peptide length of 7 amino acids. N-terminal protein acetylation and methionine oxidation were defined as variable modifications and cysteine carbamidomethylation as a fixed modification. Match between runs was activated to transfer identifications across samples based on mass and normalized retention times, with 0.7 min matching and 20 min alignment time windows. Label-free protein quantification (LFQ) was obtained with the MaxLFQ algorithm [45] with a minimum required ratio count of 1. Data analysis was performed using the Perseus software v.1.6.2.3 [46]. Data were filtered by removing proteins only identified by site, reverse hits, and potential contaminants. After the log2 transformation of LFQ intensities, biological replicates were grouped. For statistical analysis, missing data points were replaced by imputation from a normal distribution with 0.3 width and 1.8 downshift, and a two-sided two-samples *t*-test was used to identify significant protein intensity changes.

2.13. Protein enrichment analysis

LC-MS/MS data were uploaded on STRING Protein-Protein Interaction Networks Functional Enrichment Analysis version 11.5 (https://string-db.org/). Proteins uploaded were the upregulated in Post_EVs samples with difference >= 1.5 and strength >= 0.5. Full list of protein can be found in Supplementary Table 1.

2.14. iPS-cell reprogramming

Induced Pluripotent Stem Cells (iPS) were obtained from the reprogramming of human cardiac mesenchymal progenitor cells (CPC). CPC were derived as the cellular outgrowth from atrial tissue explants using an ex vivo primary tissue culture technique, as described previously [47]. The study was approved by the local Ethical Committee (Comitato Etico Cantonale, Bellinzona, Switzerland; Ref. CE 2923). For cell reprogramming into iPS, cells were infected with Sendai virus carrying OCT3/4, SOX2, KLF4, and MYC (CytoTune™-iPS 2.0 Sendai Reprogramming Kit; Thermo Fisher Scientific), as per manufacturer's instructions. A week after transduction, the medium was changed to StemFlex (Thermo Fisher Scientific). Individual colonies with embryonal stem cells (ESC)-like morphology typically appeared after 25–35 days and were transferred and expanded into Matrigel (hESC Qualified Matrix, Corning) coated wells. Established human iPS cell lines were maintained in culture in StemFlex medium.

2.15. Differentiation of iPS cells into iPS-derived cardiomyocytes (hCM)

Directed differentiation of human iPS cells into human cardiomyocytes (hCM) was performed using StemMACS™ CardioDiff Kit XF, human (Miltenyi Biotec) as per manufacturer's instructions. The medium was changed to a maintenance medium composed of RPMI 1640 with B-27 plus insulin (Thermo Fisher Scientific) at day 7. Metabolic selection of hCM was performed using a selection medium composed of RPMI 1640 without glucose (Thermo Fisher Scientific), 0.5 mg/ml human recombinant albumin, 0.2 mg/ml L-ascorbic acid 2-phosphate, and 4 mM lactate (Sigma-Aldrich) from days 10 to 17. Afterward, hCM were cultured in a maintenance medium for at least 30 days for further maturation.

2.16. hCM in vitro treatment

hCM were plated at a concentration of 60,000 cells/cm^2. Two days after the seeding cells were treated for 1hr with 2.5*10^7 particles/cm^2 of EVs isolated from plasma released before (Pre_EVs) and after (Post_EVs) exercise. To induce oxidative stress, hCM were treated with H_2O_2 (150 μM) for 1hr after EVs incubation.

2.17. EVs and hCM biochemical analysis: redox status evaluation

Cells and EVs were resuspended in PBS and sonicated twice for 10 s, with a 30-sec break, and in ice to prevent the mixture warming, using the Microson XL Model DU-2000 (Misonix Inc). Total protein content was estimated with the Bradford method [48]. Thiobarbituric acid reactive substances (TBARS) were detected as markers of lipids peroxidation, as the TBARS assay predominantly detects the intracellular level of malondialdehyde, a breakdown product of lipid peroxides [49]. The TBARS assay solution contained: 26 mM thiobarbituric acid and 15% trichloroacetic acid (TCA) in 0.25 N HCl. 50 μg of total cardiomyocyte protein were dissolved in 300 μl Milli-Q water and 600 μl of TBARS solution. The mix was incubated at 95°C for 1 h. The samples were centrifuged for 2 min at 14000 rpm, and the supernatants were analysed spectrophotometrically at 532 nm [50]. Cellular antioxidant enzymatic activity was determined by assaying Catalase (CAT), Glucose-6-Phosphate Dehydrogenase (G6PD), Glutathione Reductase (GR), and Glutathione Peroxidase (GPx) activity. 10 or 50 μg of total protein (EVs or hCM treated with EVs) were employed. CAT activity was assayed following the decomposition of H_2O_2 with a spectrophotometric analysis at 240 nm. The assay solution contained: 50 mM phosphate buffer (pH 7.0) and 5 mM H_2O_2 [51]. GR activity was assayed spectrophotometrically, following the NAPDH oxidation at 340 nm. The assay solution contained: 100 mM Tris-HCl (pH 7.4), 1 mM EDTA, 5 mM GSSH, and 0.2 mM NADPH [52]. GPx activity was assayed following the decomposition of H_2O_2 with a spectrophotometric analysis at 240 nm. The assay solution contained: 100 mM Tris-HCl (pH 7.4), 5 mM H_2O_2, and 5 mM GSH [50]. Since H_2O_2 is also a substrate of catalases, GPx activity is obtained by subtracting the result of this assay from the catalase activity values. G6PD activity was assayed following NADP reduction with a spectrophotometric analysis at 340 nm. The assay mix contained: 100 mM Tris-HCl (pH 7.4), 0.5 mM NADP, and 10 mM glucose-6-phosphate [51]. Data for all the assays were normalized on the sample protein content.

2.18. Western blot on hCM

Western blot methods for cells are the same that the ones reported for EVs. Membranes were incubated with pHAP27 (Santa Cruz Biotechnology sc-166693, 1:300), HSP27 (Santa Cruz Biotechnology sc-13132, 1:300) and GAPDH (Abcam ab181602, 1:5000).

2.19. Immunostaining

After treatment, hCM were washed twice with PBS1X and then fixed for 5 min at RT using a PFA-4% solution. Cells were then blocked and permeabilized with a solution of 2% bovine serum albumin (BSA) (Merck) + 0.3% Triton X (Triton X detergent, Sigma-Aldrich) in PBS for 1 h at RT. Subsequently, they were incubated with PBS1X containing 0.1% Triton X, 1% BSA, and the primary antibody overnight at 4°C. Cells were stained for NRF2 (Abcam ab62352; 1:200) and cardiac Troponin T (cTnT) (13-11 Thermo Fisher Scientific; 1:300). Images were acquired with Lionheart FX automatic microscopy at 10 × magnification and analysed with Gen5 software (Biotek). A first mask on cTnT-positive cells was created for the identification of cardiomyocytes; then mean fluorescent intensity (MFI) of the nuclear NRF2 signal was analysed.

2.20. RNA extraction, reverse transcription and real-time PCR

hCM were treated for 6 h with PBS, Pre_EVs and Post_EVs (hCM + PBS, hCM + Pre_EVs and hCM + Post_EVs respectively). After treatment, cells were lysed with TRI Reagent (Sigma), as per manufacturer's instructions. The pellet was air-dried, re-suspended in DEPC water, and RNA was quantified with NanoDrop™ 2000c (Thermo Fisher Scientific). RNA (500 ng) was reverse-transcribed using GoScript™ Reverse Transcription System (Promega Madison, Dubendorf, Switzerland). Real-time analysis was performed on CFX connect Bio-Rad Real-time PCR detection system (Bio-Rad). Data are shown as $2^{-\Delta\Delta Ct}$ values. Couple of primers were as follows: Human *SOD1* forward: GATGAAGAGAGGCATGTT GGAGA reverse: TTCCACCTTTGCCCAAGTCA; Human *HMOX1* forward: TCCTGGCTCAGCCTCAAATG; reverse: CACGCATGGCTCAAAAACCA; Human *CAT* forward: TGGCTTCACAAGGACTACCC; reverse: GCTGGTAGTTGGCCACTCG; Human *NQO1* forward: TGAAAGGCTGGTTTGAGCGA; reverse: AGCACTGCCTTCTTACTCCG; Human *GAPDH* forward: TGCACCACCAACTGCTTAGC Reverse: GGCATGGACTGTGGTCATGAG.

2.21. ROS detection

ROS detection was performed on EVs and cells. In EVs, ROS were measured using DCF (2',7'-dichlorofluorescein diacetate) (Thermo Fischer Scientific). Briefly, EVs were incubated with H2-DCF (2',7'-dichlorodihydrofluorescein diacetate) (100 mM) at 37°C 5%CO_2 for 30 min. The cleavage of the acetate groups by intracellular esterases and oxidation lead to the formation of DCF, a fluorescent derivative. Fluorescence was measured using a microplate reader (Tecan) at 488 nm wavelength. In cells, the cell-permeable fluorescent dye dihydroethidium (DHE) (Thermo Fischer Scientific) was used to perform ROS detection. DHE is a probe that freely permeates cell membrane and is oxidized by cellular superoxide (O_2^-) to produce two red fluorescent products, namely ethidium (E^+), which is typically formed by a non-specific redox reaction, and 2-hydroxyethidium (2-OH-E^+), a specific adduct of cellular O_2^- [53]. The fluorescent spectrum of 2-OH-E^+ (Ex 500–530 nm/Em 590–620 nm) and E^+ (Ex 520 nm/Em 610 nm) is very similar. Thus, by measuring the fluorescent signal in treated cells we estimated the global ROS levels in the sample since we can't perform a specific detection of 2-OH-E^+ (cellular O_2^- levels) due to overlapping fluorescence of 2-OH-E^+ and E^+. ROS measurement at basal conditions (hCM + PBS, hCM + Pre_EVs, and hCM + Post_EVs) was performed by adding DHE (5 μM) for 30 min (37°C 5%CO_2 in the dark) after 1hr of EVs treatment. For ROS measurement in pro-oxidant conditions (H_2O_2) DHE was added during the 30 min following 1hr of recovery after EVs and H_2O_2 treatment (1hr and 1hr respectively). At the end of the incubation time, cells were washed with PBS1X, and pictures of live cells, maintained at 37°C, were taken with Lionheart FX automatic microscopy supplemented with a heated chamber. Acquisition was performed using RFP filter (Ex 530/40 nm Em 593/40 nm) and images analysed with Gen5 software (Biotek). 100 μM of CCCP (Carbonyl cyanide 3-chlorophenylhydrazone) was used as positive control for ROS generation to set-up the analysis for further experiments. Representative images for PBS and CCCP treated cells (hCM + PBS and hCM + CCCP respectively) and schematic representation of fluorescence analysis are reported in Supplementary Fig. 2.

2.22. CCK8 viability assay

After Post_EVs and H_2O_2 treatment (1hr and 1hr respectively) medium was changed, and cells were left to recover overnight (O/N) in complete medium. Viability was measured the day later using Cell-Counting Kit-8 (CCK-8, DOJINDO). CCK-8 solution was added to the cell media and cells were incubated for a further 2–4 h at 37°C. The amount of formazan dye generated by cellular dehydrogenase activity was measured using a microplate reader (Tecan) at 450 nm wavelength.

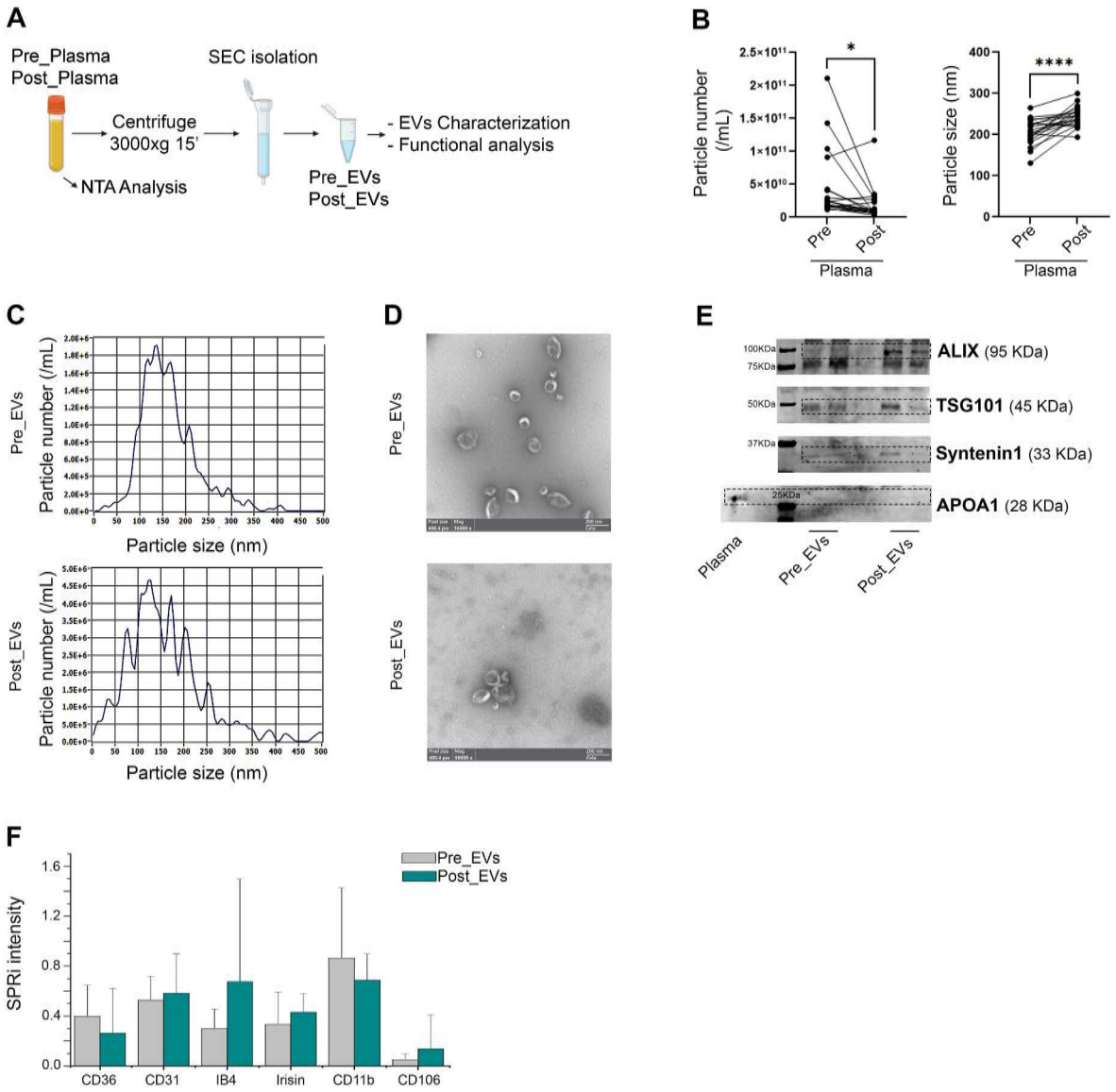

Fig. 1. A) Schematic representation of the methods B) Particles total number and diameter (nm) in plasma before isolation. Statistical significances were determined using unpaired *t*-test (*p $<$ 0.05 and ****p $<$ 0.0001); C) Representative Particle Metrix concentration and size distribution of isolated EVs; D) TEM images of Pre_EVs and Post_EVs; E) Immunoblot analysis of EVs markers and plasma contaminant; F) SPRi report.

2.23. Glutathione Reductase (GR) assay kit

The level of Glutathione Reductase (GR) activity, in hCM trated with H_2O_2 (Fig. 5D), was measured by ELISA assay (ab83461, Abcam, Cambridge, UK) following the manufacturer's instructions. Briefly, Post_EVs and H_2O_2 treated (1hr and 1hr respectively) cells were lysed by the addition of the lysis buffer provided in the kit and centrifuged at 14,000×*g* for 10 min. The GR in the supernatant reacts with DTNB to generate 2-nitro-5-thiobenzoic acid. This compound is yellow, and the sample's absorbance (405 nm) was measured by a microplate reader (TECAN). The results were normalized to total protein, measured by BCA (as previously described).

2.24. Statistical analyses

Results are shown as mean ± SEM (standard error of the mean) from >3 independent experiments. Statistical analyses of differences between 3 groups were performed by one-way ANOVA followed by post-hoc Tukey's multiple tests, and those of differences between 2 groups were performed using unpaired *t*-test with Prism Version 9 GraphPad Software. Statistical significance was defined as $p < 0.05$.

3. Results

3.1. Baseline characteristics of subjects

Young (26.95 ± 3.07 years old) and healthy males were recruited for the following study. The average estimated VO_{2max} of the volunteers was 51.22 ± 4.85 of mL/kg/min; this fitness level falls within the range of 38 $< VO_{2max} >$ 56 commonly seen in most of the physically active populations that regularly participate in nonelite sports/recreational activities [54]. All participants reported similar eating habits regarding the percentage of macro- and micronutrients consumed daily following the mediterranean diet (data not shown). Baecke Questionnaire was used to analyse daily physical activity of participants. The study protocol and the anthropometric and fitness levels of the experimental group are shown in Supplementary Fig. 1.

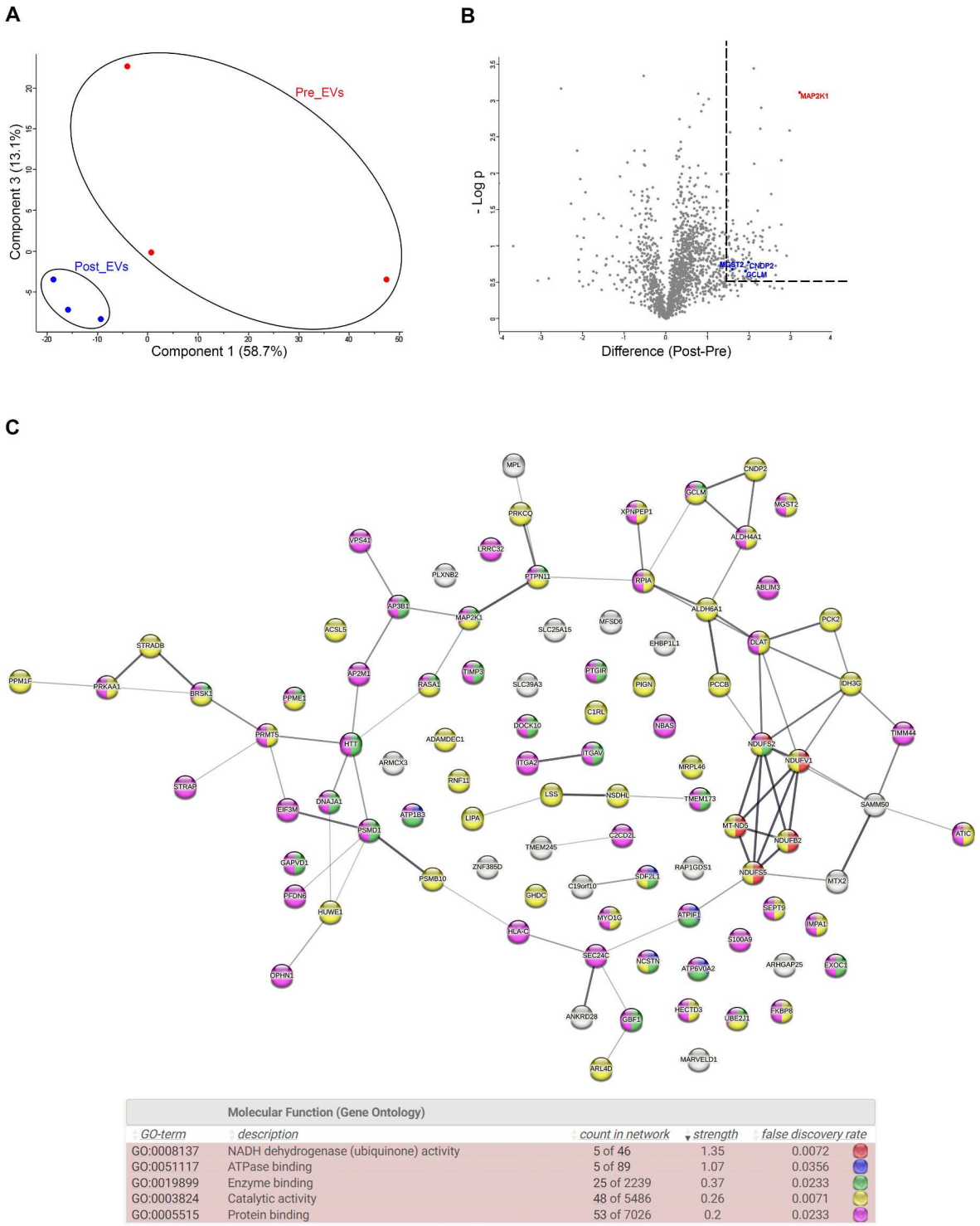

Molecular Function (Gene Ontology)				
GO-term	description	count in network	strength	false discovery rate
GO:0008137	NADH dehydrogenase (ubiquinone) activity	5 of 46	1.35	0.0072
GO:0051117	ATPase binding	5 of 89	1.07	0.0356
GO:0019899	Enzyme binding	25 of 2239	0.37	0.0233
GO:0003824	Catalytic activity	48 of 5486	0.26	0.0071
GO:0005515	Protein binding	53 of 7026	0.2	0.0233

Fig. 2. A) PCA of Pre_EVs and Post_EVs; B) Vulcano plot of differential expressed protein from Post_EVs *vs* Pre_EVs; C) Enrichment analysis of Post_EVs upregulated proteins.

3.2. A single bout of endurance exercise endurance induces changes in EVs release and cargo

Plasma collected from the 21 volunteers was cleaned from cell debris and analysed by Nanoparticle Tracking Analysis (NTA) (Fig. 1A). Collectively, all the subjects show an exercise-related decrease in the number of circulating particles with a parallel increase in size (Fig. 1B). These changes in particle number and size, prompted us to better investigate and characterize plasma-derived EVs. EVs isolated by SEC were characterized following MISEV guidelines [55]. NTA and Electron Microscopy (EM) confirmed the presence of EVs in the classically described size range (70-200 nm; Fig. 1C–D) [56,57]. Presence of small EVs (such as exosomes) in both, Pre_EVs and Post_EVs, was also confirmed by positivity for ALIX, TSG101, and Syntenin-1, well-known exosomal markers (Fig. 1E) [58]. Apolipoprotein A1 (APOA1) antibody was used to confirm the absence of contaminant lipoprotein in the EVs preparations (Fig. 1E) [59]. Finally, SPRi biosensor was used to detect multiple subpopulations of EVs in the considered plasma samples [60].

Table 1
GO analysis: molecular functional pathways.

#term ID	Term description	Observed gene count	Background gene count	Strength	False discovery rate	Matching proteins in your network (IDs)	Matching proteins in your network (labels)
GO:0008137	NADH dehydrogenase (ubiquinone) activity	5	46	1.35	0.0072	9606.ENSP00000322450,9606. ENSP00000354813,9606. ENSP00000356972,9606. ENSP00000362060,9606. ENSP00000419087	NDUFV1,MT-ND5,NDUFS2, NDUFS5,NDUFB2
GO:0051117	ATPase binding	5	89	1.07	0.0356	9606.ENSP00000248958,9606. ENSP00000286371,9606. ENSP00000294785,9606. ENSP00000332247,9606. ENSP00000335203	SDF2L1,ATP1B3,NCSTN, ATP6V0A2,ATPIF1
GO:0019899	Enzyme binding	25	2239	0.37	0.0233	9606.ENSP00000248958,9606. ENSP00000255194,9606. ENSP00000258390,9606. ENSP00000261023,9606. ENSP00000266085,9606. ENSP00000274376,9606. ENSP00000286371,9606. ENSP00000291294,9606. ENSP00000294785,9606. ENSP00000302486,9606. ENSP00000309474,9606. ENSP00000310649,9606. ENSP00000331288,9606. ENSP00000332247,9606. ENSP00000335203,9606. ENSP00000340944,9606. ENSP00000347184,9606. ENSP00000356972,9606. ENSP00000359000,9606. ENSP00000359258,9606. ENSP00000369127,9606. ENSP00000370695,9606. ENSP00000377664,9606. ENSP00000381461,9606. ENSP00000451261	SDF2L1,AP3B1,DOCK10, ITGAV,TIMP3,RASA1,ATP1B3, PTGIR,NCSTN,MAP2K1, PSMD1,BRSK1,TMEM173, ATP6V0A2,ATPIF1,PTPN11, HTT,NDUFS2,GBF1,GCLM, DNAJA1,EXOC1,GAPVD1, PPME1,UBE2J1
GO:0003824	Catalytic activity	48	5486	0.26	0.0071	9606.ENSP00000194530,9606. ENSP00000216780,9606. ENSP00000217901,9606. ENSP00000236959,9606. ENSP00000242719,9606. ENSP00000248958,9606. ENSP00000256412,9606. ENSP00000258787,9606. ENSP00000263125,9606. ENSP00000263212,9606. ENSP00000266542,9606. ENSP00000274376,9606. ENSP00000280346,9606. ENSP00000283646,9606. ENSP00000294785,9606. ENSP00000301671,9606. ENSP00000302486,9606. ENSP00000310649,9606. ENSP00000312311,9606. ENSP00000319169,9606. ENSP00000322450,9606. ENSP00000322628,9606. ENSP00000325548,9606. ENSP00000337354,9606. ENSP00000340648,9606. ENSP00000340944,9606. ENSP00000346148,9606. ENSP00000348429,9606. ENSP00000350263,9606. ENSP00000351314,9606. ENSP00000354813,9606. ENSP00000356972,9606. ENSP00000359258,9606. ENSP00000359297,9606. ENSP00000361245,9606. ENSP00000362060,9606. ENSP00000364490,9606.	STRADB,PCK2,IDH3G,ATIC, RNF11,SDF2L1,ADAMDEC1, MYO1G,PRKCQ,PPM1F,C1RL, RASA1,DLAT,RPIA,NCSTN, GHDC,MAP2K1,BRSK1, MRPL46,PRMT5,NDUFV1, ARL4D,CNDP2,LIPA,HUWE1, PTPN11,PRKAA1,ACSL5,PIGN, PSMB10,MT-ND5,NDUFS2, GCLM,NSDHL,HECTD3, NDUFS5,ALDH4A1,LSS,PPME1, SEPT9,IMPA1,PCCB,NDUFB2, XPNPEP1,ALDH6A1,UBE2J1, FKBP8,MGST2

(*continued on next page*)

Table 1 (*continued*)

#term ID	Term description	Observed gene count	Background gene count	Strength	False discovery rate	Matching proteins in your network (IDs)	Matching proteins in your network (labels)
						ENSP00000380837,9606. ENSP00000381461,9606. ENSP00000391249,9606. ENSP00000408526,9606. ENSP00000419027,9606. ENSP00000419087,9606. ENSP00000421566,9606. ENSP00000450436,9606. ENSP00000451261,9606. ENSP00000476767,9606. ENSP00000482639	
GO:0005515	Protein binding	53	7026	0.2	0.0233	9606.ENSP00000236959,9606. ENSP00000248958,9606. ENSP00000255194,9606. ENSP00000258390,9606. ENSP00000258787,9606. ENSP00000261023,9606. ENSP00000266085,9606. ENSP00000270538,9606. ENSP00000274376,9606. ENSP00000280346,9606. ENSP00000281513,9606. ENSP00000283646,9606. ENSP00000286371,9606. ENSP00000291294,9606. ENSP00000292807,9606. ENSP00000294785,9606. ENSP00000296585,9606. ENSP00000302486,9606. ENSP00000309457,9606. ENSP00000309474,9606. ENSP00000310649,9606. ENSP00000319169,9606. ENSP00000331288,9606. ENSP00000332247,9606. ENSP00000335203,9606. ENSP00000338885,9606. ENSP00000340944,9606. ENSP00000343405,9606. ENSP00000346148,9606. ENSP00000347184,9606. ENSP00000347710,9606. ENSP00000356972,9606. ENSP00000357727,9606. ENSP00000359000,9606. ENSP00000359258,9606. ENSP00000361245,9606. ENSP00000364490,9606. ENSP00000365402,9606. ENSP00000369127,9606. ENSP00000370695,9606. ENSP00000377664,9606. ENSP00000378563,9606. ENSP00000381461,9606. ENSP00000384126,9606. ENSP00000391249,9606. ENSP00000392270,9606. ENSP00000408526,9606. ENSP00000421566,9606. ENSP00000425394,9606. ENSP00000436049,9606. ENSP00000451261,9606. ENSP00000476767,9606. ENSP00000482639	ATIC,SDF2L1,AP3B1,DOCK10, MYO1G,ITGAV,TIMP3, TIMM44,RASA1,DLAT,NBAS, RPIA,ATP1B3,PTGIR,AP2M1, NCSTN,ITGA2,MAP2K1,VPS41, PSMD1,BRSK1,PRMT5, TMEM173,ATP6V0A2,ATPIF1, C2CD2L,PTPN11,SEC24C, PRKAA1,HTT,OPHN1,NDUFS2, S100A9,GBF1,GCLM,HECTD3, ALDH4A1,HLA-C,DNAJA1, EXOC1,GAPVD1,PFDN6, PPME1,LRRC32,SEPT9,STRAP, IMPA1,XPNPEP1,ABLIM3, EIF3M,UBE2J1,FKBP8,MGST2

Specific ligands for vesicles derived from adipocytes ($CD36^+$), endothelial cells ($CD31^+$, CD106+), muscle cells (Irisin+), microglia (IB4+), and activated microglia (CD11b+) were used. Due to the considerable variability, no statistically significant difference was observed between the two injected samples. However, Post_EVs showed a trend in the increase of circulating $CD31^+$ and CD106+ ($p = 0.87$) EVs, suggesting the activation of the vascular system and the release of EVs from endothelial cells, as well as increase in IB4+ and Irisin+ ($p = 0.37$ and $p = 0.25$ respectively) EVs, respectively released by microglia cells and muscles. On the contrary, a decrease in the circulating $CD36^+$ and CD11b+ ($p = 0.87$) EVs compared to Pre_EVs was registered (Fig. 1F). Principal component analysis (PCA), of proteomic data obtained from Pre and Post derived-EVs protein cargo, showed a clear separation of the analysed samples (Fig. 2A). Enrichment analysis for molecular function and

Table 2
GO analysis: biological process pathways.

#term ID	Term description	Observed gene count	Background gene count	Strength	False discovery rate	Matching proteins in your network (IDs)	Matching proteins in your network (labels)
GO:0006750	Glutathione biosynthetic process	3	14	1.65	0.0383	9606.ENSP00000325548,9606.ENSP00000359258,9606.ENSP00000482639	CNDP2,GCLM,MGST2
GO:0006120	Mitochondrial electron transport, nadh to ubiquinone	5	49	1.33	0.0371	9606.ENSP00000322450,9606.ENSP00000354813,9606.ENSP00000356972,9606.ENSP00000362060,9606.ENSP00000419087	NDUFV1,MT-ND5,NDUFS2,NDUFS5,NDUFB2
GO:0042398	Cellular modified amino acid biosynthetic process	4	45	1.27	0.0409	9606.ENSP00000236959,9606.ENSP00000325548,9606.ENSP00000359258,9606.ENSP00000482639	ATIC,CNDP2,GCLM,MGST2
GO:1903214	Regulation of protein targeting to mitochondrion	4	47	1.25	0.0416	9606.ENSP00000335203,9606.ENSP00000340648,9606.ENSP00000346148,9606.ENSP00000425394	ATPIF1,HUWE1,PRKAA1,ABLIM3
GO:0032981	Mitochondrial respiratory chain complex i assembly	5	66	1.2	0.0371	9606.ENSP00000322450,9606.ENSP00000354813,9606.ENSP00000356972,9606.ENSP00000362060,9606.ENSP00000419087	NDUFV1,MT-ND5,NDUFS2,NDUFS5,NDUFB2
GO:1903747	Regulation of establishment of protein localization to mitochondrion	5	76	1.14	0.0371	9606.ENSP00000335203,9606.ENSP00000340648,9606.ENSP00000346148,9606.ENSP00000369127,9606.ENSP00000425394	ATPIF1,HUWE1,PRKAA1,DNAJA1,ABLIM3
GO:0002474	Antigen processing and presentation of peptide antigen via mhc class i	6	96	1.11	0.0371	9606.ENSP00000261023,9606.ENSP00000309474,9606.ENSP00000343405,9606.ENSP00000351314,9606.ENSP00000365402,9606.ENSP00000376141	ITGAV,PSMD1,SEC24C,PSMB10,HLA-C,MFSD6
GO:0042590	Antigen processing and presentation of exogenous peptide antigen via mhc class i	8	80	1.11	0.0371	9606.ENSP00000261023,9606.ENSP00000309474,9606.ENSP00000351314,9606.ENSP00000365402,9606.ENSP00000376141	ITGAV,PSMD1,PSMB10,HLA-C,MFSD6
GO:0033108	Mitochondrial respiratory chain complex assembly	6	102	1.09	0.0371	9606.ENSP00000322450,9606.ENSP00000345445,9606.ENSP00000354813,9606.ENSP00000356972,9606.ENSP00000362060,9606.ENSP00000419087	NDUFV1,SAMM50,MT-ND5,NDUFS2,NDUFS5,NDUFB2
GO:0019884	Antigen processing and presentation of exogenous antigen	8	182	0.96	0.0371	9606.ENSP00000255194,9606.ENSP00000261023,9606.ENSP00000292807,9606.ENSP00000309474,9606.ENSP00000343405,9606.ENSP00000351314,9606.ENSP00000365402,9606.ENSP00000376141	AP3B1,ITGAV,AP2M1,PSMD1,SEC24C,PSMB10,HLA-C,MFSD6
GO:0045333	Cellular respiration	7	158	0.96	0.0371	9606.ENSP00000217901,9606.ENSP00000280346,9606.ENSP00000322450,9606.ENSP00000354813,9606.ENSP00000356972,9606.ENSP00000362060,9606.ENSP00000419087	IDH3G,DLAT,NDUFV1,MT-ND5,NDUFS2,NDUFS5,NDUFB2
GO:0002478	Antigen processing and presentation of exogenous peptide antigen	7	174	0.92	0.0371	9606.ENSP00000261023,9606.ENSP00000292807,9606.ENSP00000309474,9606.ENSP00000343405,9606.ENSP00000351314,9606.ENSP00000365402,9606.ENSP00000376141	ITGAV,AP2M1,PSMD1,SEC24C,PSMB10,HLA-C,MFSD6
GO:0048872	Homeostasis of number of cells	7	204	0.85	0.0383	9606.ENSP00000258390,9606.ENSP00000269740,9606.ENSP00000294785,9606.ENSP00000335203,9606.ENSP00000337354,9606.ENSP00000340944,9606.ENSP00000361548	DOCK10,SLC39A3,NCSTN,ATPIF1,LIPA,PTPN11,MPL

(*continued on next page*)

Table 2 (*continued*)

#term ID	Term description	Observed gene count	Background gene count	Strength	False discovery rate	Matching proteins in your network (IDs)	Matching proteins in your network (labels)
GO:0006091	Generation of precursor metabolites and energy	10	405	0.71	0.0371	9606.ENSP00000217901,9606. ENSP00000280346,9606. ENSP00000283646,9606. ENSP00000322450,9606. ENSP00000335203,9606. ENSP00000354813,9606. ENSP00000356972,9606. ENSP00000362060,9606. ENSP00000364490,9606. ENSP00000419087	IDH3G,DLAT,RPIA,NDUFV1, ATPIF1,MT-ND5,NDUFS2, NDUFS5,ALDH4A1,NDUFB2
GO:0007005	Mitochondrion organization	11	452	0.7	0.0371	9606.ENSP00000249442,9606. ENSP00000255194,9606. ENSP00000270538,9606. ENSP00000322450,9606. ENSP00000335203,9606. ENSP00000345445,9606. ENSP00000354813,9606. ENSP00000356972,9606. ENSP00000359258,9606. ENSP00000362060, 9606. ENSP00000419087	MTX2,AP3B1,TIMM44, NDUFV1,ATPIF1,SAMM50, MT-ND5,NDUFS2,GCLM, NDUFS5,NDUFB2
GO:0051223	Regulation of protein transport	13	617	0.64	0.0371	9606.ENSP00000263212,9606. ENSP00000335203,9606. ENSP00000338885,9606. ENSP00000340648,9606. ENSP00000340944,9606. ENSP00000346148,9606. ENSP00000347710,9606. ENSP00000369127,9606. ENSP00000370695,9606. ENSP00000377664,9606. ENSP00000384126,9606. ENSP00000425394, 9606. ENSP00000451261	PPM1F,ATPIF1,C2CD2L, HUWE1,PTPN11,PRKAA1, OPHN1,DNAJA1,EXOC1, GAPVD1,LRRC32,ABLIM3, UBE2J1
GO:1903827	Regulation of cellular protein localization	11	568	0.61	0.0416	9606.ENSP00000263212,9606. ENSP00000292807,9606. ENSP00000335203,9606. ENSP00000340648,9606. ENSP00000340944,9606. ENSP00000346148,9606. ENSP00000347710,9606. ENSP00000359000,9606. ENSP00000369127,9606. ENSP00000425394,9606. ENSP00000451261	PPM1F,AP2M1,ATPIF1, HUWE1,PTPN11,PRKAA1, OPHN1,GBF1,DNAJA1, ABLIM3,UBE2J1
GO:0032880	Regulation of protein localization	15	934	0.52	0.0371	9606.ENSP00000263212,9606. ENSP00000292807,9606. ENSP00000335203,9606. ENSP00000338885,9606. ENSP00000340648,9606. ENSP00000340944,9606. ENSP00000346148,9606. ENSP00000347710,9606. ENSP00000359000,9606. ENSP00000369127,9606. ENSP00000370695,9606. ENSP00000377664,9606. ENSP00000384126,9606. ENSP00000425394,9606. ENSP00000451261	PPM1F,AP2M1,ATPIF1, C2CD2L,HUWE1,PTPN11, PRKAA1,OPHN1,GBF1, DNAJA1,EXOC1,GAPVD1, LRRC32,ABLIM3,UBE2J1
GO:0001775	Cell activation	16	1075	0.49	0.0371	9606.ENSP00000258390,9606. ENSP00000261023,9606. ENSP00000263125,9606. ENSP00000294785,9606. ENSP00000301671,9606. ENSP00000309474,9606. ENSP00000319169,9606. ENSP00000331288,9606. ENSP00000340648,9606. ENSP00000340944,9606. ENSP00000351314,9606. ENSP00000357727,9606. ENSP00000359000,9606. ENSP00000359258,9606.	DOCK10,ITGAV,PRKCQ, NCSTN,GHDC,PSMD1, PRMT5,TMEM173,HUWE1, PTPN11,PSMB10,S100A9, GBF1,GCLM,MPL,HLA-C

(*continued on next page*)

Table 2 (*continued*)

#term ID	Term description	Observed gene count	Background gene count	Strength	False discovery rate	Matching proteins in your network (IDs)	Matching proteins in your network (labels)
						ENSP00000361548,9606. ENSP0000036540	
GO:0060341	Regulation of cellular localization	15	1027	0.48	0.046	9606.ENSP00000263212,9606. ENSP00000292807,9606. ENSP00000302486,9606. ENSP00000310649,9606. ENSP00000335203,9606. ENSP00000338885,9606. ENSP00000340648,9606. ENSP00000340944,9606. ENSP00000346148,9606. ENSP00000347184,9606. ENSP00000347710,9606. ENSP00000359000,9606. ENSP00000369127,9606. ENSP00000425394,9606. ENSP00000451261	PPM1F,AP2M1,MAP2K1, BRSK1,ATPIF1,C2CD2L, HUWE1,PTPN11,PRKAA1, HTT,OPHN1,GBF1,DNAJA1, ABLIM3,UBE2J1
GO:0140352	Export from cell	15	1028	0.48	0.046	9606.ENSP00000258787,9606. ENSP00000261023,9606. ENSP00000266085,9606. ENSP00000286371,9606. ENSP00000294785,9606. ENSP00000301671,9606. ENSP00000309457,9606. ENSP00000309474,9606. ENSP00000310649,9606. ENSP00000322628,9606. ENSP00000331288,9606. ENSP00000340648,9606. ENSP00000357727,9606. ENSP00000365402,9606. ENSP00000370695	MYO1G,ITGAV,TIMP3, ATP1B3,NCSTN,GHDC, VPS41,PSMD1,BRSK1,ARL4D, TMEM173,HUWE1,S100A9, HLA-C,EXOC1
GO:0016192	Vesicle-mediated transport	24	1805	0.44	0.0371	9606.ENSP00000255194,9606. ENSP00000258787,9606. ENSP00000261023,9606. ENSP00000266085,9606. ENSP00000281513,9606. ENSP00000292807,9606. ENSP00000294785, 9606. ENSP00000301671,9606. ENSP00000309457, 9606. ENSP00000309474,9606. ENSP00000310649,9606. ENSP00000322628,9606. ENSP00000331288,9606. ENSP00000340648,9606. ENSP00000343405,9606. ENSP00000347184,9606. ENSP00000347710,9606. ENSP00000357727, 9606. ENSP00000359000,9606. ENSP00000365402,9606. ENSP00000370695,9606. ENSP00000377664,9606. ENSP00000382379,9606. ENSP00000386911	AP3B1,MYO1G,ITGAV, TIMP3,NBAS,AP2M1,NCSTN, GHDC,VPS41,PSMD1,BRSK1, ARL4D,TMEM173,HUWE1, SEC24C,HTT,OPHN1,S100A9, GBF1,HLA-C,EXOC1,GAPVD1, ANKRD28,ARHGAP25
GO:0043085	Positive regulation of catalytic activity	19	1489	0.42	0.0409	9606.ENSP00000194530,9606. ENSP00000258390,9606. ENSP00000263125,9606. ENSP00000263212,9606. ENSP00000274376,9606. ENSP00000286371,9606. ENSP00000294785,9606. ENSP00000296585,9606. ENSP00000302486,9606. ENSP00000340454,9606. ENSP00000340944,9606. ENSP00000346148,9606. ENSP00000347710,9606. ENSP00000357727,9606. ENSP00000359258,9606. ENSP00000369127,9606. ENSP00000377664,9606.	STRADB,DOCK10,PRKCQ, PPM1F,RASA1,ATP1B3, NCSTN,ITGA2,MAP2K1, RAP1GDS1,PTPN11,PRKAA1, OPHN1,S100A9,GCLM, DNAJA1,GAPVD1, ARHGAP25,MGST2

(*continued on next page*)

Table 2 (*continued*)

#term ID	Term description	Observed gene count	Background gene count	Strength	False discovery rate	Matching proteins in your network (IDs)	Matching proteins in your network (labels)
						ENSP00000386911,9606. ENSP00000482639	
GO:0051049	Regulation of transport	21	1776	0.39	0.0414	9606.ENSP00000261023,9606. ENSP00000263212,9606. ENSP00000286371,9606. ENSP00000296585,9606. ENSP00000302486,9606. ENSP00000309457,9606. ENSP00000310649,9606. ENSP00000335203,9606. ENSP00000338885,9606. ENSP00000340648,9606. ENSP00000340944,9606. ENSP00000346148,9606. ENSP00000347184,9606. ENSP00000347710,9606. ENSP00000348429,9606. ENSP00000369127,9606. ENSP00000370695,9606. ENSP00000377664,9606. ENSP00000384126,9606. ENSP00000425394,9606. ENSP00000451261	ITGAV,PPM1F,ATP1B3, ITGA2,MAP2K1,VPS41, BRSK1,ATPIF1,C2CD2L, HUWE1,PTPN11,PRKAA1, HTT,OPHN1,ACSL5,DNAJA1, EXOC1,GAPVD1,LRRC32, ABLIM3,UBE2J1
GO:0002376	Immune system process	27	2481	0.36	0.0371	9606.ENSP00000255194,9606. ENSP00000256412,9606. ENSP00000258390,9606. ENSP00000258787,9606. ENSP00000261023,9606. ENSP00000263125,9606. ENSP00000266542,9606. ENSP00000269740,9606. ENSP00000286371,9606. ENSP00000292807,9606. ENSP00000294785,9606. ENSP00000301671,9606. ENSP00000302486,9606. ENSP00000309474,9606. ENSP00000331288,9606. ENSP00000332247,9606. ENSP00000335203,9606. ENSP00000340648,9606. ENSP00000340944,9606. ENSP00000343405,9606. ENSP00000351314,9606. ENSP00000357727,9606. ENSP00000359000,9606. ENSP00000361548,9606. ENSP00000365402,9606. ENSP00000370695,9606. ENSP00000376141	AP3B1,ADAMDEC1,DOCK10, MYO1G,ITGAV,PRKCQ,C1RL, SLC39A3,ATP1B3,AP2M1, NCSTN,GHDC,MAP2K1, PSMD1,TMEM173, ATP6V0A2,ATPIF1,HUWE1, PTPN11,SEC24C,PSMB10, S100A9,GBF1,MPL,HLA-C, EXOC1,MFSD6
GO:0050790	Regulation of catalytic activity	25	2386	0.34	0.046	9606.ENSP00000194530,9606. ENSP00000258390,9606. ENSP00000263125,9606. ENSP00000263212,9606. ENSP00000266085,9606. ENSP00000274376,9606. ENSP00000286371,9606. ENSP00000294785,9606. ENSP00000296585,9606. ENSP00000302486,9606. ENSP00000309474,9606. ENSP00000335203,9606. ENSP00000340454,9606. ENSP00000340944,9606. ENSP00000346148,9606. ENSP00000347184,9606. ENSP00000347710,9606. ENSP00000357727,9606. ENSP00000359258,9606. ENSP00000369127,9606. ENSP00000377664,9606. ENSP00000381461,9606. ENSP00000386911,9606.	STRADB,DOCK10,PRKCQ, PPM1F,TIMP3,RASA1, ATP1B3,NCSTN,ITGA2, MAP2K1,PSMD1,ATPIF1, RAP1GDS1,PTPN11,PRKAA1, HTT,OPHN1,S100A9,GCLM, DNAJA1,GAPVD1,PPME1, ARHGAP25,PLXNB2,MGST2

(*continued on next page*)

Table 2 (*continued*)

#term ID	Term description	Observed gene count	Background gene count	Strength	False discovery rate	Matching proteins in your network (IDs)	Matching proteins in your network (labels)
						ENSP00000409171,9606. ENSP00000482639	
GO:0009987	Cellular process	89	15024	0.09	0.0371	9606.ENSP00000194530,9606. ENSP00000216780,9606. ENSP00000217901,9606. ENSP00000236959,9606. ENSP00000242719,9606. ENSP00000248958,9606. ENSP00000249442,9606. ENSP00000255194,9606. ENSP00000258390, 9606. ENSP00000258787,9606. ENSP00000261023,9606. ENSP00000262947,9606. ENSP00000263125,9606. ENSP00000263212,9606. ENSP00000266085,9606. ENSP00000269740,9606. ENSP00000270538,9606. ENSP00000274376, 9606. ENSP00000280346,9606. ENSP00000281513,9606. ENSP00000283646,9606. ENSP00000286371,9606. ENSP00000291294,9606. ENSP00000292807,9606. ENSP00000294785,9606. ENSP00000296585,9606. ENSP00000301671,9606. ENSP00000302486,9606. ENSP00000309457,9606. ENSP00000309474,9606. ENSP00000310649,9606. ENSP00000312311,9606. ENSP00000312671,9606. ENSP00000319169,9606. ENSP00000322450,9606. ENSP00000322628,9606. ENSP00000325548,9606. ENSP00000331288,9606. ENSP00000332247,9606. ENSP00000335203,9606. ENSP00000337354,9606. ENSP00000338885,9606. ENSP00000340454,9606. ENSP00000340648,9606. ENSP00000340672,9606. ENSP00000340944,9606. ENSP00000342267,9606. ENSP00000343405,9606. ENSP00000345445,9606. ENSP00000346148,9606. ENSP00000347184,9606. ENSP00000347710,9606. ENSP00000348429,9606. ENSP00000350263,9606. ENSP00000351314,9606. ENSP00000354813,9606. ENSP00000356972,9606. ENSP00000357727,9606. ENSP00000359000,9606. ENSP00000359258,9606. ENSP00000359297, 9606. ENSP00000361245,9606. ENSP00000361548,9606. ENSP00000362060,9606. ENSP00000364490,9606. ENSP00000365402,9606. ENSP00000369127,9606. ENSP00000370695,9606. ENSP00000377664,9606. ENSP00000378563,9606. ENSP00000380837,9606. ENSP00000381461,9606.	STRADB,PCK2,IDH3G,ATIC, RNF11,SDF2L1,MTX2,AP3B1, DOCK10,MYO1G,ITGAV, C19orf10,PRKCQ,PPM1F, TIMP3,SLC39A3,TIMM44, RASA1,DLAT,NBAS,RPIA, ATP1B3,PTGIR,AP2M1, NCSTN,ITGA2,GHDC, MAP2K1,VPS41,PSMD1, BRSK1,MRPL46,EHBP1L1, PRMT5,NDUFV1,ARL4D, CNDP2,TMEM173, ATP6V0A2,ATPIF1,LIPA, C2CD2L,RAP1GDS1,HUWE1, ARMCX3,PTPN11,SLC25A15, SEC24C,SAMM50,PRKAA1, HTT,OPHN1,ACSL5,PIGN, PSMB10,MT-ND5,NDUFS2, S100A9,GBF1,GCLM,NSDHL, HECTD3,MPL,NDUFS5, ALDH4A1,HLA-C,DNAJA1, EXOC1,GAPVD1,PFDN6,LSS, PPME1,ANKRD28,LRRC32, ARHGAP25,SEPT9,STRAP, IMPA1,PLXNB2,PCCB, NDUFB2,XPNPEP1,ABLIM3, EIF3M,MARVELD1,ALDH6A1, UBE2J1,FKBP8,MGST2

(*continued on next page*)

Table 2 (*continued*)

#term ID	Term description	Observed gene count	Background gene count	Strength	False discovery rate	Matching proteins in your network (IDs)	Matching proteins in your network (labels)
						ENSP00000382379,9606. ENSP00000384126,9606. ENSP00000386911,9606. ENSP00000391249,9606. ENSP00000392270,9606. ENSP00000408526,9606. ENSP00000409171,9606. ENSP00000419027,9606. ENSP00000419087,9606. ENSP00000421566,9606. ENSP00000425394,9606. ENSP00000436049,9606. ENSP00000441365,9606. ENSP00000450436,9606. ENSP00000451261,9606. ENSP00000476767,9606. ENSP00000482639	

biological process on the most upregulated proteins in Post_EVs (difference >= 1.5 and strength >= 0.5; Fig. 2B; full proteins list Supplementary Table 1), evidenced enrichment in proteins with a function in the maintenance of cells energetic balance (Table 1 and Table 2; Fig. 2C). These data were supported by cellular component enrichment analysis (Table 3) that confirmed upregulation of mitochondrial proteins, in Post_EVs. To note, 48 of the 98 upregulated proteins have catalytic activity, as by Gene Ontology (GO) analysis (Fig. 2C). Among them, the most significatively upregulated protein is the well-known mitogen-activated protein kinase kinase 1 (MAP2K1), a kinase with different known roles, even in oxidative stress damage response [61]. Interestingly, Post_EVs showed significative increased levels of carnosine dipeptidase 2 (CNDP2), glutamate-cysteine ligase modifier subunit (GCLM), and microsomal glutathione S-transferase 2 (MGST2) (Fig. 2B) three protein essential for the glutathione biosynthetic process (Table 2). Biosynthesis of glutathione plays a key role in the antioxidant response [62]. Despite protein expression level of Glutathione Reductase (GR) and Catalase (CAT), two key antioxidant enzymes, was not significatively different between Pre and Post derived-EVs (difference Post_EVs vs Pre_EVs 0.4 and -0.14 respectively, Supplementary Table 1), the biochemical assessment of their activity showed that both GR and CAT were more active in Post_EVs compared to Pre_EVs (Fig. 3A). It is known that the enzymatic activity of both is upregulated following PE [63] in order to protect cells against increased H_2O_2 formation [64]. In agreement with this, Post_EVs showed lower levels of ROS compared to Pre_EVs (Fig. 3B). Globally, these data suggested that Post_EVs have greater antioxidant activity.

3.3. Post_EVs induce activation of antioxidant and cardioprotective pathways on hCM

Isolated Pre_EVs and Post_EVs were then used to perform functional analysis on human iPS-derived cardiomyocytes (hCM). Vesicles were added on top of cultured cells. After 1hr of treatment, hCM were collected to perform analysis of AOEs activity. Both GR and CAT resulted more active in hCM treated with Post_EVs (hCM + Post_EVs) compared to Pre_EVs treated (hCM + Pre_EVs) and not treated cells (hCM + PBS) (Fig. 3C). Furthermore, additional analysis showed that hCM + Post_EVs had increased activity of glutathione peroxidase (GPx) and glucose 6-phosphate dehydrogenase (G6PD) (Fig. 3C); other two fundamental players in the antioxidant response [65]. Interestingly, lipid peroxidation was significantly downregulated in EVs-treated hCM, with Post_EVs resulting more potent than Pre_EVs (Fig. 3D). The decrease in global ROS levels by Post_EVs was also confirmed with DHE (Dihydroethidium) analysis (Fig. 3E). Among the known signalling pathways involved in oxidative stress reduction, in cardiomyocytes, activation of HSP27 (Heat shock protein 27) has a central role [66,67]. Interestingly, it has been previously shown that EVs are able to activate HSP27 phosphorylation with consequent cardioprotection [68]. In accordance with the previous data here, we found that Post_EVs were able to significantly increase HSP27 phosphorylation in treated cardiomyocytes (Fig. 4A). Since Post_EVs showed to be able to induce the activation of different antioxidant enzymes, we decided to perform nuclear translocation analysis on NRF2 (Nuclear factor erythroid 2-related factor 2). Immunofluorescence analysis on hCM treated with Pre- or Post-derived EVs showed an increase in NRF2 nuclear translocation after Post_EVs treatment (Fig. 4B). Furthermore, the downstream effect of NRF2 nuclear translocation was confirmed by RT-Realtime-PCR analysis on treated hCM, 6 h post EVs exposure. In accordance with the immunofluorescence results, we found that Post_EVs were able to significatively increase the transcription of *SOD1* and *HMOX1* genes, while only a positive trend was observed for *CAT* and *NQO1* (Supplementary Fig. 3).

3.4. Post_EVs protect cardiomyocytes from oxidative stress

Since Post_EVs resulted to be able to activate protective and antioxidant pathways in cardiomyocytes, we decided to investigate their protective role in pro-oxidant conditions. hCM were treated with 150 μM of H_2O_2 for 1hr. The selected dose was able to induce a significant increase in ROS production resulting in hCM cell death of about 50% (Fig. 5A). Post_EVs were used to treat hCM 1 h before H_2O_2 treatment. EVs isolated from plasma obtained post-physical exercise decrease ROS levels in hCM under pro-oxidant conditions (Fig. 5B) and improve cell viability (Fig. 5C). Furthermore, a biochemical assay on GR activity, showed an increase in this enzyme functionality following Post_EVs treatment (Fig. 5D).

4. Discussion

While there are several work showing how EVs, in particular the one derived from stem and progenitor cells can protect target cells against oxidative stress [69,70], in this study, we demonstrated, for the first time, that EVs released in the circulation immediately after a single endurance exercise have beneficial effect. Specifically, here we showed that EVs released immediately after a single endurance exercise (Post_EVs), by healthy young males with a high average fitness level, exert antioxidant and cardioprotective effects in human-induced cardiomyocyte (hCM) *in vitro* model. It is known that physical exercise induces EVs release and changes in their cargo [20]. In particular, acute exercise causes large EVs release in circulation, also known as microvesicles (MVs), which can be a carrier of a huge number of proteins altered after exercise [21]. In line with that, our NTA analysis showed a

Table 3
GO analysis: cellular component.

#term ID	Term description	Observed gene count	Background gene count	Strength	False discovery rate	Matching proteins in your network (IDs)	Matching proteins in your network (labels)
GO:0005747	Mitochondrial respiratory chain complex i	5	48	1.34	0.0023	9606.ENSP00000322450,9606.ENSP00000354813,9606.ENSP00000356972,9606.ENSP00000362060,9606.ENSP00000419087	NDUFV1,MT-ND5,NDUFS2,NDUFS5,NDUFB2
GO:1990204	Oxidoreductase complex	6	107	1.07	0.0029	9606.ENSP00000280346,9606.ENSP00000322450,9606.ENSP00000354813,9606.ENSP00000356972,9606.ENSP00000362060,9606.ENSP00000419087	DLAT,NDUFV1,MT-ND5,NDUFS2,NDUFS5,NDUFB2
GO:0098798	Mitochondrial protein complex	9	262	0.85	0.0023	9606.ENSP00000249442,9606.ENSP00000280346,9606.ENSP00000312311,9606.ENSP00000322450,9606.ENSP00000345445,9606.ENSP00000354813,9606.ENSP00000356972,9606.ENSP00000362060,9606.ENSP00000419087	MTX2,DLAT,MRPL46,NDUFV1,SAMM50,MT-ND5,NDUFS2,NDUFS5,NDUFB2
GO:0031966	Mitochondrial membrane	14	722	0.61	0.0023	9606.ENSP00000249442,9606.ENSP00000270538,9606.ENSP00000312311,9606.ENSP00000322450,9606.ENSP00000331288,9606.ENSP00000340672,9606.ENSP00000342267,9606.ENSP00000345445,9606.ENSP00000348429,9606.ENSP00000354813,9606.ENSP00000356972,9606.ENSP00000362060,9606.ENSP00000419087,9606.ENSP00000476767	MTX2,TIMM44,MRPL46,NDUFV1,TMEM173,ARMCX3,SLC25A15,SAMM50,ACSL5,MT-ND5,NDUFS2,NDUFS5,NDUFB2,FKBP8
GO:0005759	Mitochondrial matrix	9	479	0.59	0.0344	9606.ENSP00000216780,9606.ENSP00000217901,9606.ENSP00000270538,9606.ENSP00000280346,9606.ENSP00000312311,9606.ENSP00000356972,9606.ENSP00000364490,9606.ENSP00000419027,9606.ENSP00000450436	PCK2,IDH3G,TIMM44,DLAT,MRPL46,NDUFS2,ALDH4A1,PCCB,ALDH6A1
GO:0005739	Mitochondrion	28	1611	0.56	1.20E-06	9606.ENSP00000216780,9606.ENSP00000217901,9606.ENSP00000249442,9606.ENSP00000255194,9606.ENSP00000270538,9606.ENSP00000280346,9606.ENSP00000294785,9606.ENSP00000302486,9606.ENSP00000312311,9606.ENSP00000322450,9606.ENSP00000331288,9606.ENSP00000335203,9606.ENSP00000340454,9606.ENSP00000340672,9606.ENSP00000340944,9606.ENSP00000342267,9606.ENSP00000345445,9606.ENSP00000348429,9606.ENSP00000354813,9606.ENSP00000356972,9606.ENSP00000359000,9606.ENSP00000362060,9606.ENSP00000364490,9606.ENSP00000369127,9606.ENSP00000419027,9606.ENSP00000419087,9606.ENSP00000450436,9606.ENSP00000476767	PCK2,IDH3G,MTX2,AP3B1,TIMM44,DLAT,NCSTN,MAP2K1,MRPL46,NDUFV1,TMEM173,ATPIF1,RAP1GDS1,ARMCX3,PTPN11,SLC25A15,SAMM50,ACSL5,MT-ND5,NDUFS2,GBF1,NDUFS5,ALDH4A1,DNAJA1,PCCB,NDUFB2,ALDH6A1,FKBP8

(*continued on next page*)

Table 3 (*continued*)

#term ID	Term description	Observed gene count	Background gene count	Strength	False discovery rate	Matching proteins in your network (IDs)	Matching proteins in your network (labels)
GO:0098796	Membrane protein complex	17	1141	0.49	0.0044	9606.ENSP00000249442,9606. ENSP00000255194,9606. ENSP00000261023,9606. ENSP00000286371,9606. ENSP00000292807,9606. ENSP00000294785,9606. ENSP00000296585,9606. ENSP00000309457,9606. ENSP00000322450,9606. ENSP00000332247,9606. ENSP00000343405,9606. ENSP00000345445,9606. ENSP00000354813,9606. ENSP00000356972,9606. ENSP00000362060,9606. ENSP00000365402,9606. ENSP00000419087	MTX2,AP3B1,ITGAV,ATP1B3, AP2M1,NCSTN,ITGA2,VPS41, NDUFV1,ATP6V0A2,SEC24C, SAMM50,MT-ND5,NDUFS2, NDUFS5,HLA-C,NDUFB2
GO:0031967	Organelle envelope	17	1213	0.46	0.008	9606.ENSP00000249442,9606. ENSP00000270538,9606. ENSP00000301671,9606. ENSP00000312311,9606. ENSP00000322450,9606. ENSP00000331288,9606. ENSP00000340672,9606. ENSP00000342267,9606. ENSP00000345445,9606. ENSP00000348429,9606. ENSP00000354813,9606. ENSP00000356972,9606. ENSP00000361548,9606. ENSP00000362060,9606. ENSP00000419087,9606. ENSP00000476767,9606. ENSP00000482639	MTX2,TIMM44,GHDC,MRPL46, NDUFV1,TMEM173,ARMCX3, SLC25A15,SAMM50,ACSL5, MT-ND5,NDUFS2,MPL, NDUFS5,NDUFB2,FKBP8, MGST2
GO:0005789	Endoplasmic reticulum membrane	14	1085	0.43	0.043	9606.ENSP00000248958,9606. ENSP00000281513,9606. ENSP00000331288,9606. ENSP00000338885,9606. ENSP00000343405,9606. ENSP00000348429,9606. ENSP00000350263,9606. ENSP00000359297,9606. ENSP00000365402,9606. ENSP00000369127,9606. ENSP00000380837,9606. ENSP00000451261,9606. ENSP00000476767,9606. ENSP00000482639	SDF2L1,NBAS,TMEM173, C2CD2L,SEC24C,ACSL5,PIGN, NSDHL,HLA-C,DNAJA1,LSS, UBE2J1,FKBP8,MGST2
GO:0031090	Organelle membrane	35	3548	0.31	0.0023	9606.ENSP00000248958,9606. ENSP00000249442,9606. ENSP00000255194,9606. ENSP00000261023,9606. ENSP00000270538,9606. ENSP00000281513,9606. ENSP00000292807,9606. ENSP00000294785,9606. ENSP00000309457,9606. ENSP00000312311,9606. ENSP00000322450,9606. ENSP00000331288,9606. ENSP00000332247,9606. ENSP00000338885,9606. ENSP00000340672,9606. ENSP00000342267,9606. ENSP00000343405,9606. ENSP00000345445,9606. ENSP00000347184,9606. ENSP00000348429,9606. ENSP00000350263,9606. ENSP00000354813,9606. ENSP00000356972,9606. ENSP00000359000,9606. ENSP00000359297,9606. ENSP00000361548,9606.	SDF2L1,MTX2,AP3B1,ITGAV, TIMM44,NBAS,AP2M1,NCSTN, VPS41,MRPL46,NDUFV1, TMEM173,ATP6V0A2,C2CD2L, ARMCX3,SLC25A15,SEC24C, SAMM50,HTT,ACSL5,PIGN, MT-ND5,NDUFS2,GBF1, NSDHL,MPL,NDUFS5,HLA-C, DNAJA1,LSS,ANKRD28, NDUFB2,UBE2J1,FKBP8, MGST2

(*continued on next page*)

Table 3 (*continued*)

#term ID	Term description	Observed gene count	Background gene count	Strength	False discovery rate	Matching proteins in your network (IDs)	Matching proteins in your network (labels)
						ENSP00000362060,9606. ENSP00000365402,9606. ENSP00000369127,9606. ENSP00000380837,9606. ENSP00000382379,9606. ENSP00000419087,9606. ENSP00000451261,9606. ENSP00000476767,9606. ENSP00000482639	
GO:0005829	Cytosol	42	5193	0.23	0.0106	9606.ENSP00000194530,9606. ENSP00000216780,9606. ENSP00000236959,9606. ENSP00000258390,9606. ENSP00000261023,9606. ENSP00000263125,9606. ENSP00000263212,9606. ENSP00000274376,9606. ENSP00000281513,9606. ENSP00000283646,9606. ENSP00000291294,9606. ENSP00000292807,9606. ENSP00000302486,9606. ENSP00000309457,9606. ENSP00000309474,9606. ENSP00000319169,9606. ENSP00000322450,9606. ENSP00000325548,9606. ENSP00000331288,9606. ENSP00000340454,9606. ENSP00000340648,9606. ENSP00000340944,9606. ENSP00000343405,9606. ENSP00000346148,9606. ENSP00000347184,9606. ENSP00000347710,9606. ENSP00000350263,9606. ENSP00000351314,9606. ENSP00000357727,9606. ENSP00000359000,9606. ENSP00000359258,9606. ENSP00000369127,9606. ENSP00000370695,9606. ENSP00000377664,9606. ENSP00000382379,9606. ENSP00000386911,9606. ENSP00000392270,9606. ENSP00000408526,9606. ENSP00000419027,9606. ENSP00000421566,9606. ENSP00000436049,9606. ENSP00000476767	STRADB,PCK2,ATIC,DOCK10, ITGAV,PRKCQ,PPM1F,RASA1, NBAS,RPIA,PTGIR,AP2M1, MAP2K1,VPS41,PSMD1, PRMT5,NDUFV1,CNDP2, TMEM173,RAP1GDS1,HUWE1, PTPN11,SEC24C,PRKAA1,HTT, OPHN1,PIGN,PSMB10,S100A9, GBF1,GCLM,DNAJA1,EXOC1, GAPVD1,ANKRD28, ARHGAP25,STRAP,IMPA1, PCCB,XPNPEP1,EIF3M,FKBP8
GO:0012505	Endomembrane system	37	4542	0.23	0.026	9606.ENSP00000242719,9606. ENSP00000248958,9606. ENSP00000255194,9606. ENSP00000261023,9606. ENSP00000262947,9606. ENSP00000266085,9606. ENSP00000281513,9606. ENSP00000292807,9606. ENSP00000294785,9606. ENSP00000301671,9606. ENSP00000302486,9606. ENSP00000309457,9606. ENSP00000309474,9606. ENSP00000310649,9606. ENSP00000312671,9606. ENSP00000319169,9606. ENSP00000331288,9606. ENSP00000332247,9606. ENSP00000338885,9606. ENSP00000340454,9606. ENSP00000340648,9606. ENSP00000343405,9606. ENSP00000347184,9606.	RNF11,SDF2L1,AP3B1,ITGAV, C19orf10,TIMP3,NBAS,AP2M1, NCSTN,GHDC,MAP2K1,VPS41, PSMD1,BRSK1,EHBP1L1, PRMT5,TMEM173,ATP6V0A2, C2CD2L,RAP1GDS1,HUWE1, SEC24C,HTT,ACSL5,PIGN, S100A9,GBF1,NSDHL,MPL, HLA-C,DNAJA1,GAPVD1,LSS, ANKRD28,UBE2J1,FKBP8, MGST2

(*continued on next page*)

Table 3 (*continued*)

#term ID	Term description	Observed gene count	Background gene count	Strength	False discovery rate	Matching proteins in your network (IDs)	Matching proteins in your network (labels)
						ENSP00000348429,9606. ENSP00000350263,9606. ENSP00000357727,9606. ENSP00000359000,9606. ENSP00000359297,9606. ENSP00000361548,9606. ENSP00000365402,9606. ENSP00000369127,9606. ENSP00000377664,9606. ENSP00000380837,9606. ENSP00000382379,9606. ENSP00000451261,9606. ENSP00000476767,9606. ENSP00000482639	
GO:0032991	Protein-containing complex	40	5073	0.22	0.026	9606.ENSP00000242719,9606. ENSP00000248958,9606. ENSP00000249442,9606. ENSP00000255194,9606. ENSP00000258787,9606. ENSP00000261023,9606. ENSP00000263212,9606. ENSP00000280346,9606. ENSP00000281513,9606. ENSP00000286371,9606. ENSP00000292807,9606. ENSP00000294785,9606. ENSP00000296585,9606. ENSP00000309457,9606. ENSP00000309474,9606. ENSP00000312311,9606. ENSP00000312671,9606. ENSP00000319169,9606. ENSP00000322450,9606. ENSP00000332247,9606. ENSP00000335203,9606. ENSP00000340944,9606. ENSP00000343405,9606. ENSP00000345445,9606. ENSP00000346148,9606. ENSP00000347184,9606. ENSP00000351314,9606. ENSP00000354813,9606. ENSP00000356972,9606. ENSP00000359258,9606. ENSP00000362060,9606. ENSP00000365402,9606. ENSP00000370695,9606. ENSP00000378563,9606. ENSP00000391249,9606. ENSP00000392270,9606. ENSP00000409171,9606. ENSP00000419087,9606. ENSP00000436049,9606. ENSP00000476767	RNF11,SDF2L1,MTX2,AP3B1, MYO1G,ITGAV,PPM1F,DLAT, NBAS,ATP1B3,AP2M1,NCSTN, ITGA2,VPS41,PSMD1,MRPL46, EHBP1L1,PRMT5,NDUFV1, ATP6V0A2,ATPIF1,PTPN11, SEC24C,SAMM50,PRKAA1, HTT,PSMB10,MT-ND5, NDUFS2,GCLM,NDUFS5,HLA- C,EXOC1,PFDN6,SEPT9, STRAP,PLXNB2,NDUFB2, EIF3M,FKBP8
GO:0005737	Cytoplasm	83	11428	0.18	4.15E-07	9606.ENSP00000194530,9606. ENSP00000216780,9606. ENSP00000217901,9606. ENSP00000236959,9606. ENSP00000242719,9606. ENSP00000248958,9606. ENSP00000249442,9606. ENSP00000255194,9606. ENSP00000258390,9606. ENSP00000258787,9606. ENSP00000261023,9606. ENSP00000262947,9606. ENSP00000263125,9606. ENSP00000263212,9606. ENSP00000266085,9606. ENSP00000270538,9606. ENSP00000274376,9606. ENSP00000280346,9606. ENSP00000281513,9606. ENSP00000283646,9606.	STRADB,PCK2,IDH3G,ATIC, RNF11,SDF2L1,MTX2,AP3B1, DOCK10,MYO1G,ITGAV, C19orf10,PRKCQ,PPM1F, TIMP3,TIMM44,RASA1,DLAT, NBAS,RPIA,ATP1B3,PTGIR, AP2M1,NCSTN,ITGA2,GHDC, MAP2K1,VPS41,PSMD1,BRSK1, MRPL46,EHBP1L1,PRMT5, NDUFV1,ARL4D,CNDP2, TMEM173,ATP6V0A2,ATPIF1, LIPA,C2CD2L,RAP1GDS1, HUWE1,ARMCX3,PTPN11, SLC25A15,SEC24C,SAMM50, PRKAA1,HTT,OPHN1,ACSL5, PIGN,PSMB10,MT-ND5, NDUFS2,S100A9,GBF1,GCLM, NSDHL,HECTD3,MPL,NDUFS5, ALDH4A1,HLA-C,DNAJA1, EXOC1,GAPVD1,PFDN6,

(*continued on next page*)

Table 3 (*continued*)

#term ID	Term description	Observed gene count	Background gene count	Strength	False discovery rate	Matching proteins in your network (IDs)	Matching proteins in your network (labels)
						ENSP00000286371,9606. ENSP00000291294,9606. ENSP00000292807,9606. ENSP00000294785,9606. ENSP00000296585,9606. ENSP00000301671,9606. ENSP00000302486,9606. ENSP00000309457,9606. ENSP00000309474,9606. ENSP00000310649,9606. ENSP00000312311,9606. ENSP00000312671,9606. ENSP00000319169,9606. ENSP00000322450,9606. ENSP00000322628,9606. ENSP00000325548,9606. ENSP00000331288,9606. ENSP00000332247,9606. ENSP00000335203,9606. ENSP00000337354,9606. ENSP00000338885,9606. ENSP00000340454,9606. ENSP00000340648,9606. ENSP00000340672,9606. ENSP00000340944,9606. ENSP00000342267,9606. ENSP00000343405,9606. ENSP00000345445,9606. ENSP00000346148,9606. ENSP00000347184,9606. ENSP00000347710,9606. ENSP00000348429,9606. ENSP00000350263,9606. ENSP00000351314,9606. ENSP00000354813,9606. ENSP00000356972,9606. ENSP00000357727,9606. ENSP00000359000,9606. ENSP00000359258,9606. ENSP00000359297,9606. ENSP00000361245,9606. ENSP00000361548,9606. ENSP00000362060,9606. ENSP00000364490,9606. ENSP00000365402,9606. ENSP00000369127,9606. ENSP00000370695,9606. ENSP00000377664,9606. ENSP00000378563,9606. ENSP00000382379,9606. ENSP00000386911,9606. ENSP00000391249,9606. ENSP00000392270,9606. ENSP00000408526,9606. ENSP00000419027,9606. ENSP00000419087,9606. ENSP00000421566,9606. ENSP00000425394,9606. ENSP00000436049,9606. ENSP00000441365,9606. ENSP00000450436,9606. ENSP00000476767,9606. ENSP00000482639	ANKRD28,ARHGAP25,SEPT9, STRAP,IMPA1,PCCB,NDUFB2, XPNPEP1,ABLIM3,EIF3M, MARVELD1,ALDH6A1,FKBP8, MGST2
GO:0016020	Membrane	60	9072	0.14	0.0335	9606.ENSP00000236959,9606. ENSP00000248958,9606. ENSP00000249442,9606. ENSP00000255194,9606. ENSP00000258390,9606. ENSP00000258787,9606. ENSP00000261023,9606. ENSP00000263125,9606. ENSP00000269740,9606. ENSP00000270538,9606. ENSP00000274376,9606.	ATIC,SDF2L1,MTX2,AP3B1, DOCK10,MYO1G,ITGAV, PRKCQ,SLC39A3,TIMM44, RASA1,NBAS,ATP1B3,PTGIR, AP2M1,NCSTN,ITGA2,GHDC, MAP2K1,VPS41,PSMD1, MRPL46,EHBP1L1,NDUFV1, ARL4D,TMEM173,ATP6V0A2, C2CD2L,HUWE1,ARMCX3, SLC25A15,SEC24C,SAMM50, PRKAA1,HTT,ACSL5,PIGN,MT-

(*continued on next page*)

Table 3 (*continued*)

#term ID	Term description	Observed gene count	Background gene count	Strength	False discovery rate	Matching proteins in your network (IDs)	Matching proteins in your network (labels)
						ENSP00000281513,9606. ENSP00000286371,9606. ENSP00000291294,9606. ENSP00000292807,9606. ENSP00000294785,9606. ENSP00000296585,9606. ENSP00000301671,9606. ENSP00000302486,9606. ENSP00000309457,9606. ENSP00000309474,9606. ENSP00000312311,9606. ENSP00000312671,9606. ENSP00000322450,9606. ENSP00000322628,9606. ENSP00000331288,9606. ENSP00000332247,9606. ENSP00000338885,9606. ENSP00000340648,9606. ENSP00000340672,9606. ENSP00000342267,9606. ENSP00000343405,9606. ENSP00000345445,9606. ENSP00000346148,9606. ENSP00000347184,9606. ENSP00000348429,9606. ENSP00000350263,9606. ENSP00000354813,9606. ENSP00000356972,9606. ENSP00000357727,9606. ENSP00000359000,9606. ENSP00000359297,9606. ENSP00000361548,9606. ENSP00000362060,9606. ENSP00000363714,9606. ENSP00000365402,9606. ENSP00000369127,9606. ENSP00000370695,9606. ENSP00000376141,9606. ENSP00000377664,9606. ENSP00000380837,9606. ENSP00000382379,9606. ENSP00000384126,9606. ENSP00000386911,9606. ENSP00000409171,9606. ENSP00000419087,9606. ENSP00000441365,9606. ENSP00000451261,9606. ENSP00000476767,9606. ENSP00000482639	ND5,NDUFS2,S100A9,GBF1, NSDHL,MPL,NDUFS5, TMEM245,HLA-C,DNAJA1, EXOC1,MFSD6,GAPVD1,LSS, ANKRD28,LRRC32,ARHGAP25, PLXNB2,NDUFB2,MARVELD1, UBE2J1,FKBP8,MGST2
GO:0005622	Intracellular	88	14276	0.11	0.00021	9606.ENSP00000194530,9606. ENSP00000216780,9606. ENSP00000217901,9606. ENSP00000236959,9606. ENSP00000242719,9606. ENSP00000248958,9606. ENSP00000249442,9606. ENSP00000255194,9606. ENSP00000258390,9606. ENSP00000258787,9606. ENSP00000261023,9606. ENSP00000262947,9606. ENSP00000263125,9606. ENSP00000263212,9606. ENSP00000266085,9606. ENSP00000270538,9606. ENSP00000274376,9606. ENSP00000280346,9606. ENSP00000281513,9606. ENSP00000281523,9606. ENSP00000283646,9606. ENSP00000286371,9606. ENSP00000291294,9606. ENSP00000292807,9606. ENSP00000294785,9606.	STRADB,PCK2,IDH3G,ATIC, RNF11,SDF2L1,MTX2,AP3B1, DOCK10,MYO1G,ITGAV, C19orf10,PRKCQ,PPM1F, TIMP3,TIMM44,RASA1,DLAT, NBAS,ZNF385D,RPIA,ATP1B3, PTGIR,AP2M1,NCSTN,ITGA2, GHDC,MAP2K1,VPS41,PSMD1, BRSK1,MRPL46,EHBP1L1, PRMT5,NDUFV1,ARL4D, CNDP2,TMEM173,ATP6V0A2, ATPIF1,LIPA,C2CD2L, RAP1GDS1,HUWE1,ARMCX3, PTPN11,SLC25A15,SEC24C, SAMM50,PRKAA1,HTT, OPHN1,ACSL5,PIGN,PSMB10, MT-ND5,NDUFS2,S100A9, GBF1,GCLM,NSDHL,HECTD3, MPL,NDUFS5,ALDH4A1,HLA- C,DNAJA1,EXOC1,GAPVD1, PFDN6,LSS,PPME1,ANKRD28, LRRC32,ARHGAP25,SEPT9, STRAP,IMPA1,PCCB,NDUFB2, XPNPEP1,ABLIM3,EIF3M,

(*continued on next page*)

Table 3 (*continued*)

#term ID	Term description	Observed gene count	Background gene count	Strength	False discovery rate	Matching proteins in your network (IDs)	Matching proteins in your network (labels)
						ENSP00000296585,9606. ENSP00000301671,9606. ENSP00000302486,9606. ENSP00000309457,9606. ENSP00000309474,9606. ENSP00000310649,9606. ENSP00000312311,9606. ENSP00000312671,9606. ENSP00000319169,9606. ENSP00000322450,9606. ENSP00000322628,9606. ENSP00000325548,9606. ENSP00000331288,9606. ENSP00000332247,9606. ENSP00000335203,9606. ENSP00000337354,9606. ENSP00000338885,9606. ENSP00000340454,9606. ENSP00000340648,9606. ENSP00000340672,9606. ENSP00000340944,9606. ENSP00000342267,9606. ENSP00000343405,9606. ENSP00000345445,9606. ENSP00000346148,9606. ENSP00000347184,9606. ENSP00000347710,9606. ENSP00000348429,9606. ENSP00000350263,9606. ENSP00000351314,9606. ENSP00000354813,9606. ENSP00000356972,9606. ENSP00000357727,9606. ENSP00000359000,9606. ENSP00000359258,9606. ENSP00000359297,9606. ENSP00000361245,9606. ENSP00000361548,9606. ENSP00000362060,9606. ENSP00000364490,9606. ENSP00000365402,9606. ENSP00000369127,9606. ENSP00000370695,9606. ENSP00000377664,9606. ENSP00000378563,9606. ENSP00000380837,9606. ENSP00000381461,9606. ENSP00000382379,9606. ENSP00000384126,9606. ENSP00000386911,9606. ENSP00000391249,9606. ENSP00000392270,9606. ENSP00000408526,9606. ENSP00000419027,9606. ENSP00000419087,9606. ENSP00000421566,9606. ENSP00000425394,9606. ENSP00000436049,9606. ENSP00000441365,9606. ENSP00000450436,9606. ENSP00000451261,9606. ENSP00000476767,9606. ENSP00000482639	MARVELD1,ALDH6A1,UBE2J1, FKBP8,MGST2
GO:0043227	Membrane-bounded organelle	77	12427	0.11	0.0082	9606.ENSP00000194530,9606. ENSP00000216780,9606. ENSP00000217901,9606. ENSP00000236959,9606. ENSP00000242719,9606. ENSP00000248958,9606. ENSP00000249442,9606. ENSP00000255194,9606. ENSP00000258390,9606. ENSP00000258787,9606. ENSP00000261023,9606.	STRADB,PCK2,IDH3G,ATIC, RNF11,SDF2L1,MTX2,AP3B1, DOCK10,MYO1G,ITGAV, C19orf10,PPM1F,TIMP3,C1RL, TIMM44,DLAT,NBAS, ZNF385D,RPIA,ATP1B3, AP2M1,NCSTN,ITGA2,GHDC, MAP2K1,VPS41,PSMD1,BRSK1, MRPL46,EHBP1L1,PRMT5, NDUFV1,ARL4D,CNDP2, TMEM173,ATP6V0A2,ATPIF1,

(*continued on next page*)

Table 3 (*continued*)

#term ID	Term description	Observed gene count	Background gene count	Strength	False discovery rate	Matching proteins in your network (IDs)	Matching proteins in your network (labels)
						ENSP00000262947,9606. ENSP00000263212,9606. ENSP00000266085,9606. ENSP00000266542,9606. ENSP00000270538,9606. ENSP00000280346,9606. ENSP00000281513,9606. ENSP00000281523,9606. ENSP00000283646,9606. ENSP00000286371,9606. ENSP00000292807,9606. ENSP00000294785,9606. ENSP00000296585,9606. ENSP00000301671,9606. ENSP00000302486,9606. ENSP00000309457,9606. ENSP00000309474,9606. ENSP00000310649,9606. ENSP00000312311,9606. ENSP00000312671,9606. ENSP00000319169,9606. ENSP00000322450,9606. ENSP00000322628,9606. ENSP00000325548,9606. ENSP00000331288,9606. ENSP00000332247,9606. ENSP00000335203,9606. ENSP00000337354,9606. ENSP00000338885,9606. ENSP00000340454,9606. ENSP00000340648,9606. ENSP00000340672,9606. ENSP00000340944,9606. ENSP00000342267,9606. ENSP00000343405,9606. ENSP00000345445,9606. ENSP00000346148,9606. ENSP00000347184,9606. ENSP00000348429,9606. ENSP00000350263,9606. ENSP00000351314,9606. ENSP00000354813,9606. ENSP00000356972,9606. ENSP00000357727,9606. ENSP00000359000,9606. ENSP00000359297,9606. ENSP00000361548,9606. ENSP00000362060,9606. ENSP00000364490,9606. ENSP00000365402,9606. ENSP00000369127,9606. ENSP00000377664,9606. ENSP00000380837,9606. ENSP00000381461,9606. ENSP00000382379,9606. ENSP00000384126,9606. ENSP00000392270,9606. ENSP00000409171,9606. ENSP00000419027,9606. ENSP00000419087,9606. ENSP00000421566,9606. ENSP00000441365,9606. ENSP00000450436,9606. ENSP00000451261,9606. ENSP00000476767,9606. ENSP00000482639	LIPA,C2CD2L,RAP1GDS1, HUWE1,ARMCX3,PTPN11, SLC25A15,SEC24C,SAMM50, PRKAA1,HTT,ACSL5,PIGN, PSMB10,MT-ND5,NDUFS2, S100A9,GBF1,NSDHL,MPL, NDUFS5,ALDH4A1,HLA-C, DNAJA1,GAPVD1,LSS,PPME1, ANKRD28,LRRC32,STRAP, PLXNB2,PCCB,NDUFB2, XPNPEP1,MARVELD1, ALDH6A1,UBE2J1,FKBP8, MGST2
GO:0043226	Organelle	81	13515	0.1	0.0101	9606.ENSP00000194530,9606. ENSP00000216780,9606. ENSP00000217901,9606. ENSP00000236959,9606. ENSP00000242719,9606. ENSP00000248958,9606. ENSP00000249442,9606. ENSP00000255194,9606.	STRADB,PCK2,IDH3G,ATIC, RNF11,SDF2L1,MTX2,AP3B1, DOCK10,MYO1G,ITGAV, C19orf10,PRKCQ,PPM1F, TIMP3,C1RL,TIMM44,DLAT, NBAS,ZNF385D,RPIA,ATP1B3, AP2M1,NCSTN,ITGA2,GHDC, MAP2K1,VPS41,PSMD1,BRSK1,

(*continued on next page*)

Table 3 (*continued*)

#term ID	Term description	Observed gene count	Background gene count	Strength	False discovery rate	Matching proteins in your network (IDs)	Matching proteins in your network (labels)
						ENSP00000258390,9606. ENSP00000258787,9606. ENSP00000261023,9606. ENSP00000262947,9606. ENSP00000263125,9606. ENSP00000263212,9606. ENSP00000266085,9606. ENSP00000266542,9606. ENSP00000270538,9606. ENSP00000280346,9606. ENSP00000281513,9606. ENSP00000281523,9606. ENSP00000283646,9606. ENSP00000286371,9606. ENSP00000292807,9606. ENSP00000294785,9606. ENSP00000296585,9606. ENSP00000301671,9606. ENSP00000302486,9606. ENSP00000309457,9606. ENSP00000309474,9606. ENSP00000310649,9606. ENSP00000312311,9606. ENSP00000312671,9606. ENSP00000319169,9606. ENSP00000322450,9606. ENSP00000322628,9606. ENSP00000325548,9606. ENSP00000331288,9606. ENSP00000332247,9606. ENSP00000335203,9606. ENSP00000337354,9606. ENSP00000338885,9606. ENSP00000340454,9606. ENSP00000340648,9606. ENSP00000340672,9606. ENSP00000340944,9606. ENSP00000342267,9606. ENSP00000343405,9606. ENSP00000345445,9606. ENSP00000346148,9606. ENSP00000347184,9606. ENSP00000347710,9606. ENSP00000348429,9606. ENSP00000350263,9606. ENSP00000351314,9606. ENSP00000354813,9606. ENSP00000356972,9606. ENSP00000357727,9606. ENSP00000359000,9606. ENSP00000359297,9606. ENSP00000361548,9606. ENSP00000362060,9606. ENSP00000364490,9606. ENSP00000365402,9606. ENSP00000369127,9606. ENSP00000377664,9606. ENSP00000380837,9606. ENSP00000381461,9606. ENSP00000382379,9606. ENSP00000384126,9606. ENSP00000391249,9606. ENSP00000392270,9606. ENSP00000409171,9606. ENSP00000419027,9606. ENSP00000419087,9606. ENSP00000421566,9606. ENSP00000425394,9606. ENSP00000441365,9606. ENSP00000450436,9606. ENSP00000451261,9606. ENSP00000476767,9606. ENSP00000482639	MRPL46,EHBP1L1,PRMT5, NDUFV1,ARL4D,CNDP2, TMEM173,ATP6V0A2,ATPIF1, LIPA,C2CD2L,RAP1GDS1, HUWE1,ARMCX3,PTPN11, SLC25A15,SEC24C,SAMM50, PRKAA1,HTT,OPHN1,ACSL5, PIGN,PSMB10,MT-ND5, NDUFS2,S100A9,GBF1,NSDHL, MPL,NDUFS5,ALDH4A1,HLA- C,DNAJA1,GAPVD1,LSS, PPME1,ANKRD28,LRRC32, SEPT9,STRAP,PLXNB2,PCCB, NDUFB2,XPNPEP1,ABLIM3, MARVELD1,ALDH6A1,UBE2J1, FKBP8,MGST2

(*continued on next page*)

Table 3 (*continued*)

#term ID	Term description	Observed gene count	Background gene count	Strength	False discovery rate	Matching proteins in your network (IDs)	Matching proteins in your network (labels)
GO:0043229	Intracellular organelle	76	12528	0.1	0.0233	9606.ENSP00000194530,9606. ENSP00000216780,9606. ENSP00000217901,9606. ENSP00000242719,9606. ENSP00000248958,9606. ENSP00000249442,9606. ENSP00000255194,9606. ENSP00000258390,9606. ENSP00000258787,9606. ENSP00000261023,9606. ENSP00000262947,9606. ENSP00000263125,9606. ENSP00000263212,9606. ENSP00000266085,9606. ENSP00000270538,9606. ENSP00000280346,9606. ENSP00000281513,9606. ENSP00000281523,9606. ENSP00000283646,9606. ENSP00000286371,9606. ENSP00000292807,9606. ENSP00000294785,9606. ENSP00000296585,9606. ENSP00000301671,9606. ENSP00000302486,9606. ENSP00000309457,9606. ENSP00000309474,9606. ENSP00000310649,9606. ENSP00000312311,9606. ENSP00000312671,9606. ENSP00000319169,9606. ENSP00000322450,9606. ENSP00000322628,9606. ENSP00000325548,9606. ENSP00000331288,9606. ENSP00000332247,9606. ENSP00000335203,9606. ENSP00000337354,9606. ENSP00000338885,9606. ENSP00000340454,9606. ENSP00000340648,9606. ENSP00000340672,9606. ENSP00000340944,9606. ENSP00000342267,9606. ENSP00000343405,9606. ENSP00000345445,9606. ENSP00000346148,9606. ENSP00000347184,9606. ENSP00000347710,9606. ENSP00000348429,9606. ENSP00000351314,9606. ENSP00000354813,9606. ENSP00000356972,9606. ENSP00000357727,9606. ENSP00000359000,9606. ENSP00000359297,9606. ENSP00000361548,9606. ENSP00000362060,9606. ENSP00000364490,9606. ENSP00000365402,9606. ENSP00000369127,9606. ENSP00000377664,9606. ENSP00000380837,9606. ENSP00000381461,9606. ENSP00000382379,9606. ENSP00000384126,9606. ENSP00000391249,9606. ENSP00000392270,9606. ENSP00000419027,9606. ENSP00000419087,9606. ENSP00000425394,9606. ENSP00000441365,9606. ENSP00000450436,9606. ENSP00000451261,9606.	STRADB,PCK2,IDH3G,RNF11, SDF2L1,MTX2,AP3B1,DOCK10, MYO1G,ITGAV,C19orf10, PRKCQ,PPM1F,TIMP3, TIMM44,DLAT,NBAS, ZNF385D,RPIA,ATP1B3, AP2M1,NCSTN,ITGA2,GHDC, MAP2K1,VPS41,PSMD1,BRSK1, MRPL46,EHBP1L1,PRMT5, NDUFV1,ARL4D,CNDP2, TMEM173,ATP6V0A2,ATPIF1, LIPA,C2CD2L,RAP1GDS1, HUWE1,ARMCX3,PTPN11, SLC25A15,SEC24C,SAMM50, PRKAA1,HTT,OPHN1,ACSL5, PSMB10,MT-ND5,NDUFS2, S100A9,GBF1,NSDHL,MPL, NDUFS5,ALDH4A1,HLA-C, DNAJA1,GAPVD1,LSS,PPME1, ANKRD28,LRRC32,SEPT9, STRAP,PCCB,NDUFB2,ABLIM3, MARVELD1,ALDH6A1,UBE2J1, FKBP8,MGST2

(*continued on next page*)

Table 3 (*continued*)

#term ID	Term description	Observed gene count	Background gene count	Strength	False discovery rate	Matching proteins in your network (IDs)	Matching proteins in your network (labels)
						ENSP00000476767,9606. ENSP00000482639	
GO:0110165	Cellular anatomical entity	94	17788	0.04	0.0107	9606.ENSP00000194530,9606. ENSP00000216780,9606. ENSP00000217901,9606. ENSP00000236959,9606. ENSP00000242719,9606. ENSP00000248958,9606. ENSP00000249442,9606. ENSP00000255194,9606. ENSP00000256412,9606. ENSP00000258390,9606. ENSP00000258787,9606. ENSP00000261023,9606. ENSP00000262947,9606. ENSP00000263125,9606. ENSP00000263212,9606. ENSP00000266085,9606. ENSP00000266542,9606. ENSP00000269740,9606. ENSP00000270538,9606. ENSP00000274376,9606. ENSP00000280346,9606. ENSP00000281513,9606. ENSP00000281523,9606. ENSP00000283646,9606. ENSP00000286371,9606. ENSP00000291294,9606. ENSP00000292807,9606. ENSP00000294785,9606. ENSP00000296585,9606. ENSP00000301671,9606. ENSP00000302486,9606. ENSP00000309457,9606. ENSP00000309474,9606. ENSP00000310649,9606. ENSP00000312311,9606. ENSP00000312671,9606. ENSP00000319169,9606. ENSP00000322450,9606. ENSP00000322628,9606. ENSP00000325548,9606. ENSP00000331288,9606. ENSP00000332247,9606. ENSP00000335203,9606. ENSP00000337354,9606. ENSP00000338885,9606. ENSP00000340454,9606. ENSP00000340648,9606. ENSP00000340672,9606. ENSP00000340944,9606. ENSP00000342267,9606. ENSP00000343405,9606. ENSP00000345445,9606. ENSP00000346148,9606. ENSP00000347184,9606. ENSP00000347710,9606. ENSP00000348429,9606. ENSP00000350263,9606. ENSP00000351314,9606. ENSP00000354813,9606. ENSP00000356972,9606. ENSP00000357727,9606. ENSP00000359000,9606. ENSP00000359258,9606. ENSP00000359297,9606. ENSP00000361245,9606. ENSP00000361548,9606. ENSP00000362060,9606. ENSP00000363714,9606. ENSP00000364490,9606. ENSP00000365402,9606. ENSP00000369127,9606. ENSP00000370695,9606.	STRADB,PCK2,IDH3G,ATIC, RNF11,SDF2L1,MTX2,AP3B1, ADAMDEC1,DOCK10,MYO1G, ITGAV,C19orf10,PRKCQ, PPM1F,TIMP3,C1RL,SLC39A3, TIMM44,RASA1,DLAT,NBAS, ZNF385D,RPIA,ATP1B3,PTGIR, AP2M1,NCSTN,ITGA2,GHDC, MAP2K1,VPS41,PSMD1,BRSK1, MRPL46,EHBP1L1,PRMT5, NDUFV1,ARL4D,CNDP2, TMEM173,ATP6V0A2,ATPIF1, LIPA,C2CD2L,RAP1GDS1, HUWE1,ARMCX3,PTPN11, SLC25A15,SEC24C,SAMM50, PRKAA1,HTT,OPHN1,ACSL5, PIGN,PSMB10,MT-ND5, NDUFS2,S100A9,GBF1,GCLM, NSDHL,HECTD3,MPL,NDUFS5, TMEM245,ALDH4A1,HLA-C, DNAJA1,EXOC1,MFSD6, GAPVD1,PFDN6,LSS,PPME1, ANKRD28,LRRC32,ARHGAP25, SEPT9,STRAP,IMPA1,PLXNB2, PCCB,NDUFB2,XPNPEP1, ABLIM3,EIF3M,MARVELD1, ALDH6A1,UBE2J1,FKBP8, MGST2

(*continued on next page*)

Table 3 (*continued*)

#term ID	Term description	Observed gene count	Background gene count	Strength	False discovery rate	Matching proteins in your network (IDs)	Matching proteins in your network (labels)
						ENSP00000376141,9606.	
						ENSP00000377664,9606.	
						ENSP00000378563,9606.	
						ENSP00000380837,9606.	
						ENSP00000381461,9606.	
						ENSP00000382379,9606.	
						ENSP00000384126,9606.	
						ENSP00000386911,9606.	
						ENSP00000391249,9606.	
						ENSP00000392270,9606.	
						ENSP00000408526,9606.	
						ENSP00000409171,9606.	
						ENSP00000419027,9606.	
						ENSP00000419087,9606.	
						ENSP00000421566,9606.	
						ENSP00000425394,9606.	
						ENSP00000436049,9606.	
						ENSP00000441365,9606.	
						ENSP00000450436,9606.	
						ENSP00000451261,9606.	
						ENSP00000476767,9606.	
						ENSP00000482639	

significant slight increase in particle size in plasma obtained immediately after PE. Together with the size increase, we also showed a decrease in the total number of particles. This is in contrast with what was already reported in the literature [20,71]. However, we need to consider that circulating EVs total number can change in function of PE protocols and depends also on sex, age, and pathophysiological condition [72]. Moreover, it has been reported that oxidative stress can lead to MVBs (multi-vesicular bodies) degradation with consequent release of exosomes by stressed cells [73–75]. Since PE induces a general reduction in oxidative stress [76,77], we can hypothesize that our observed increase in size and decrease in the number of circulating particles could be due to a global decrease in the stress level of producing cells. Furthermore, it is important to underline that, to avoid any possible isolation bias, this is the only reported study in which NTA was performed directly on plasma, and not on isolated EVs. Taken together, these findings confirmed that 30 min of endurance exercise are enough to modulate the EVs release [21] and induced us to better investigate the role and cargo of these EVs. Characterization of isolated particles following the MISEV guidelines [MISEV] confirmed the presence of EVs in our preparation. SPRi analysis showed a trend in the increase of Irisin + EVs, suggesting the activation of skeletal muscle tissue in the release of EVs, as expected since the previously known paracrine role of muscle tissue [21,78]. We also observed a slight increase in $CD31^+$ and CD106+ EVs, in Post_EVs samples compared to the Pre_EVs, suggesting an active role of the vascular system in EVs release, following PE [31]. It is known that one of the major vascular adaptations to exercise training is the increase in the endothelial cell nitric oxide (NO) synthase (eNOS) expression [79], a known cardioprotective molecule [80]. Furthermore, several studies report the cardioprotective role of endothelial cells-derived EVs [81,82]. However, it is important to underline that 99.8% of EVs in circulation are derived from blood cells and just 0.2% from other tissue [83]. In particular, studies based on large-EVs cell--specific antigens showed that EVs produced during physical exercise were mainly released by PBMCs, platelets, and red blood cells (RBC) [84,85]. Interestingly, RBC-derived EVs are enriched in AOEs [86]. Since our proteomic analysis showed the presence of AOEs and the biochemical assays demonstrate an increase in GR and CAT activity on EVs obtained from plasma after PE, we can speculate that plasma obtained immediately after acute exercise is enriched in EVs released by RBC. Enrichment analysis on the most upregulated proteins in EV_Post highlights the enrichment in protein with catalytic, enzyme binding, and ATPase binding activity, as reported by GO. Moreover, we found significative increase of CNDP2, GCLM, and MGST2 presence, three proteins essential in the glutathione biosynthetic process. Globally, our enzymatic and proteomic data, suggested a greater reducing potential of Post_EVs, compared to Pre_EVs. These data were confirmed by Post_EVs decreased ROS levels. The hypothesis of a reducing effect exerted by Post_EVs was also supported by functional tests using isolated EVs to treat hCM, *in vitro*. hCM treated for 1 h by Post_EVs showed significant increase in CAT, GR, G6PD, and GPx activity, compared to both untreated and Pre_EVs treated cells. Greater activity of AOEs was also confirmed by a decrease of ROS and TBAR levels in Post_EVs treated cells. To note, in this work, we wanted to demonstrate a general modulation in ROS levels, without focusing on a specific species. As a matter of fact, the use of DHE probe to evaluate ROS levels through fluorescent analysis does not allow to fully distinguish between different ROS species. Indeed, 2-OH-E^+, the product of DHE following reaction with O_2^-, and E^+, the product of DHE following non-specific redox reaction, have a similar fluorescent spectrum, that can't be separated using our analysis. Further studies, using more specific readout techniques, such as liquid chromatography–mass spectrometry (LC–MS), could allow accurate quantification of 2-OH-E^+ and consequently of O_2^- levels in the analysed cells [87]. Taken together all these results confirm that EVs released post aerobic PE were able to modulate the mechanism involved in redox homeostasis maintaining in hCM.

Interestingly, treatment with Post_EVs was also able to induce a fast and significative phosphorylation of HSP27 on treated hCM. HSP27 is a small HSPs well known for its cardioprotective role [64] that was demonstrated to function as antioxidant protein during oxidative stress [67]. Furthermore, we demonstrated that Post_EVs treatment was able to induce NRF2 nuclear translocation in hCM. NRF2 is one of the main transcription factors of AOEs expression [88]. It is important to specify that the fast antioxidant effect that we observed on hCM treated with Post_EVs was mainly due to the catalytic activity exerted by the EVs' protein cargo and not by de novo synthesis of AOEs induced by NRF2 nuclear translocations [89]. However, our analysis on hCM, 6hr after Post_EVs treatment, showed significant increase in mRNA levels of *SOD1* and *HMOX1,* two well-known NRF2 target gens [90]. These data confirm that NRF2 nuclear translocation induced by Post_EVs treatment can modulate oxidative homeostasis in target cells activating their defence mechanisms through the increase of antioxidant enzymes expression [91,92]. Finally, the antioxidant effect of Post_EVs was also demonstrated in pro-oxidant conditions. hCM treated with a sublethal dose of H_2O_2 showed a significant decrease in ROS concentration with

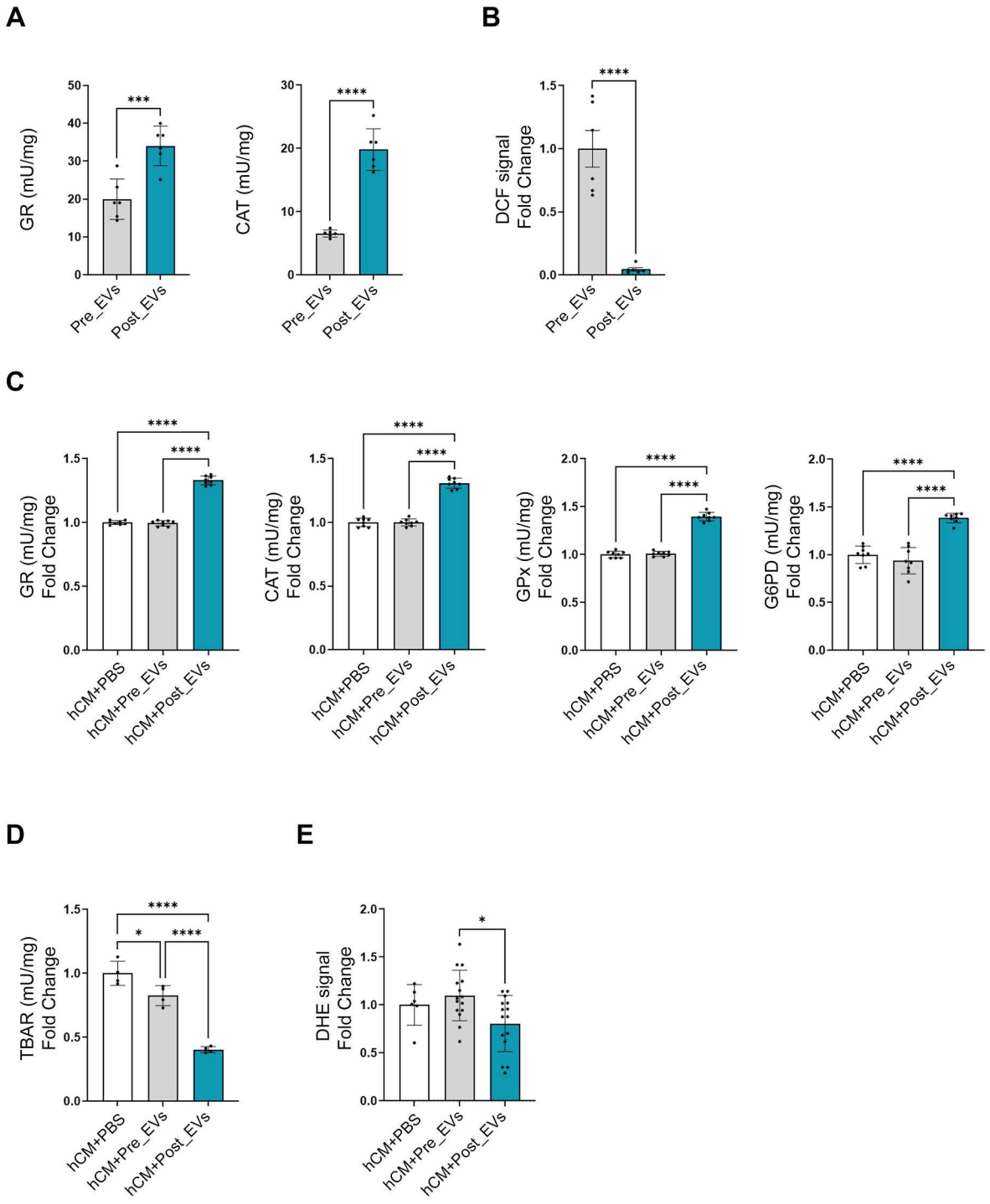

Fig. 3. A) Analysis of GR and CAT activity on Pre_EVs and Post_EVs; B) ROS concentration (measured as DCF fluorescent signal) on Pre_EVs and Post_EVs; Statistical significances were determined using unpaired *t*-test (***$p < 0.001$, ****$p < 0.0001$). C) analysis of GR, CAT, GPx and G6PD activity in hCM + PBS, hCM + Pre_EVs and hCM + Post_EVs; D) TBARS levels in hCM + PBS, hCM + Pre_EVs and hCM + Post_EVs; E) ROS concentrations (measured as DHE fluorescent signal) in hCM + PBS, hCM + Pre_EVs and hCM + Post_EVs; Statistical significance were determined using one-way anova (*$p < 0.05$,****$p < 0.0001$).

consequent improvement in cell viability when pre-treated with Post_EVs. Taken together these data confirmed a general cardioprotective effect of Post_EVs in both basal and stress conditions.

5. Conclusions

In conclusion, given all the results, with the limitation that the study was conducted on EVs derived only from male subjects, here we hypothesize that EVs released immediately after an acute bout of aerobic exercise have redox capacity in the short term, with the direct transfer of their antioxidant cargo as well as antioxidant enzymes. Proteomic analysis on EVs showed significant upregulation of MAP2K1 in Post_EVs which can explain the rapid phosphorylation of HSP27. However, further studies are needed to evaluate the long-term effect of EVs treatment in cardioprotection. With our data, we can only hypothesize a beneficial effect on hCM, in the long term, due to NRF2 nuclear translocation that leads to de novo synthesis of AOEs.

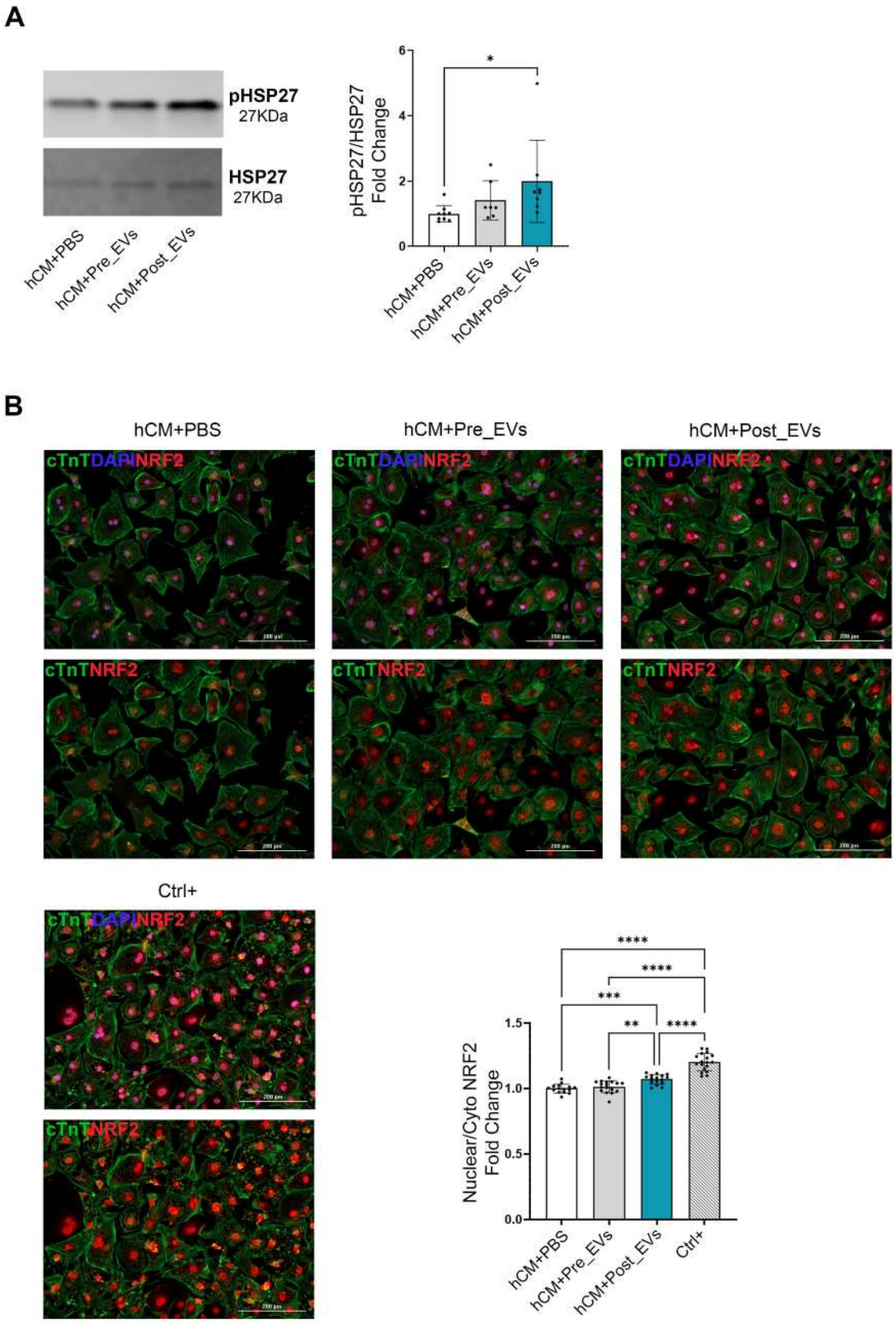

Fig. 4. A) pHSP27 immunoblot analysis on hCM + PBS, hCM + Pre_EVs and hCM + Post_EVs. B) Representative images of hCM + PBS, hCM + Pre_EVs, hCM + Post_EVs and Ctrl+ (hCM treated with H2O2) immunostained for NRF2 (red), cardiac-troponin T (cTnT-green) and DAPI; On the right panel, quantification of NRF2 nuclear translocation. Statistical significance were determined using one-way anova (*$p < 0.05$, **$p < 0.01$, ***$p < 0.001$, ****$p < 0.0001$). (For interpretation of the references to colour in this figure legend, the reader is referred to the Web version of this article.)

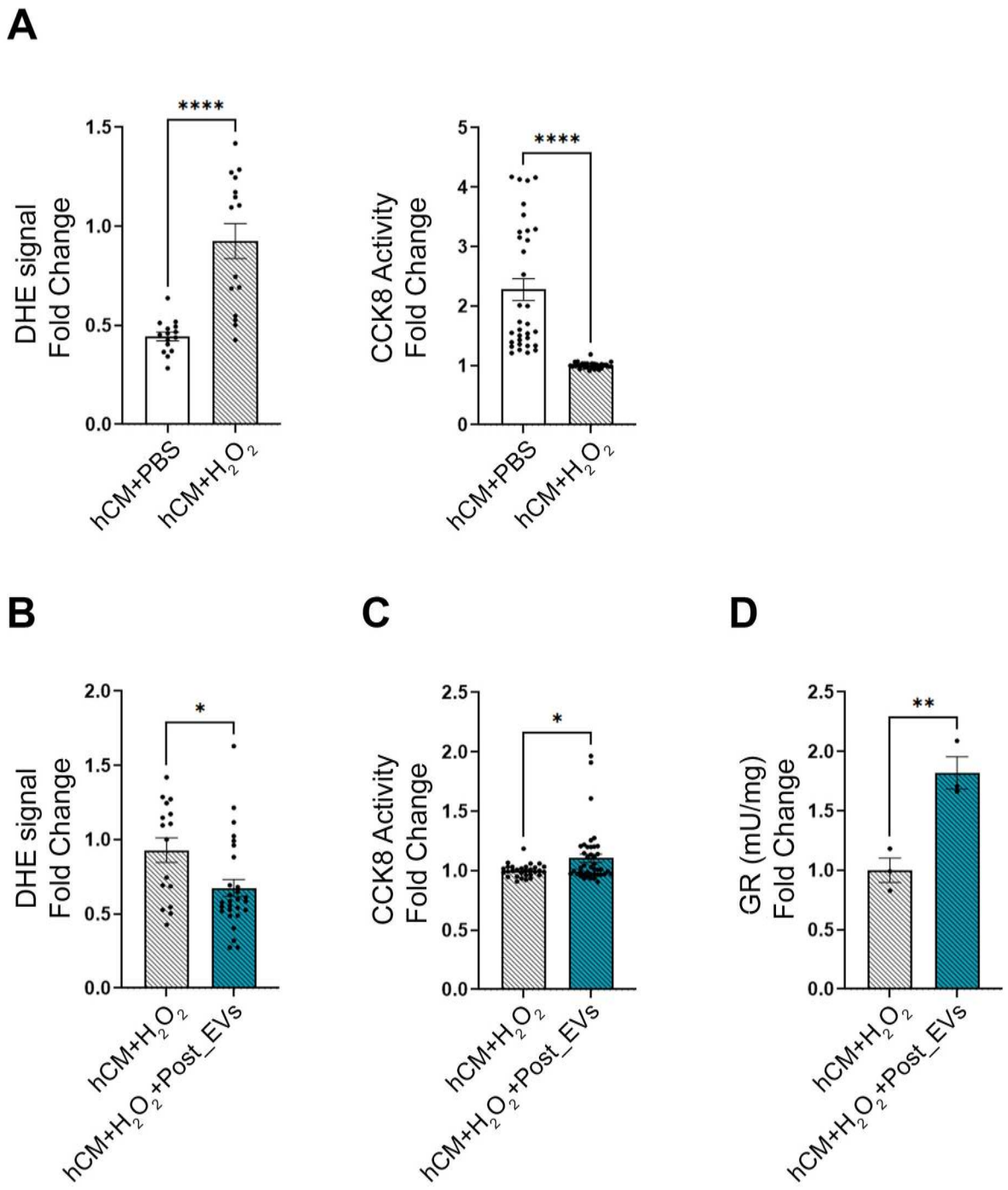

Fig. 5. A) ROS concentrations (measured as DHE fluorescent signal) and Viability (measured as CCK8 activity) analysis on hCM + PBS *vs* hCM + H_2O_2; B) ROS concentrations (measured as DHE fluorescent signal) in hCM + H_2O_2 *vs* hCM + H_2O_2+Post_EVs; C) Vitality (measured as CCK8 activity) analysis in hCM + H_2O_2 *vs* hCM + H_2O_2+Post_EVs; D) GR activity in hCM + H_2O_2 *vs* hCM + H_2O_2+Post_EVs; Statistical significances were determined using unpaired *t*-test (*$p < 0.05$, **$p < 0.01$,****$p < 0.0001$).

Author's contribution

V.L. Data generation and interpretation, manuscript writing and final approval; G.S data generation and interpretation, manuscript final approval, N.B. Biochemical data generation, manuscript final approval; M.P. Proteomic data generation, manuscript final approval; S.B. Technical assistance, manuscript final approval; A.G. SPRi data generation and interpretation, manuscript final approval; S.P. SPRi data generation and interpretation, manuscript final approval; A.R. E.M. data generation and interpretation, manuscript final approval; E.M. A.P. physical fitness level evaluation; endurance exercise protocol and manuscript final approval; C.F. P.S. L. DiL. Subjects blood collection, medical assistance, and manuscript final approval; S.R. Biochemical data interpretation, manuscript final approval; G.V Data interpretation, manuscript writing and final approval; D.C. Study design, data interpretation, manuscript writing and final approval; C.B. Study design, data interpretation, manuscript writing and final approval.

Declaration of competing interest

Authors declare no conflict of interest.

Data availability

Data will be made available on request.

Acknowledgments

This work was supported by Swiss Heart Foundation grant number FF22021 to C.B. and by Foro Italico University grant H83C23000140001 to D.C.

Appendix A. Supplementary data

Supplementary data to this article can be found online at https://doi.org/10.1016/j.redox.2023.102737.

References

[1] H.M. Ahmed, M.J. Blaha, K. Nasir, J.J. Rivera, R.S. Blumenthal, Effects of physical activity on cardiovascular disease, Am. J. Cardiol. 109 (2) (Jan. 2012) 288–295, https://doi.org/10.1016/j.amjcard.2011.08.042.

[2] D.E.R. Warburton, S.S.D. Bredin, Health benefits of physical activity: a systematic review of current systematic reviews, Curr. Opin. Cardiol. 32 (5) (Sep. 2017) 541–556, https://doi.org/10.1097/HCO.0000000000000437.

[3] M. Gleeson, N.C. Bishop, D.J. Stensel, M.R. Lindley, S.S. Mastana, M.A. Nimmo, The anti-inflammatory effects of exercise: mechanisms and implications for the prevention and treatment of disease, Nat. Rev. Immunol. 11 (9) (Sep. 2011) 607–615, https://doi.org/10.1038/nri3041.

[4] K. Pinckard, K.K. Baskin, K.I. Stanford, Effects of exercise to improve cardiovascular health, Front. Cardiovasc. Med. 6 (Jun. 2019) 69, https://doi.org/10.3389/fcvm.2019.00069.

[5] A.S.-Y. Kong, K.S. Lai, C.-W. Hee, J.Y. Loh, S.H.E. Lim, M. Sathiya, Oxidative stress parameters as biomarkers of cardiovascular disease towards the development and progression, Antioxidants 11 (6) (Jun. 2022), 1175, https://doi.org/10.3390/antiox11061175.

[6] U. Hink, et al., Mechanisms underlying endothelial dysfunction in diabetes mellitus, Circ. Res. 88 (2) (Feb. 2001), https://doi.org/10.1161/01.RES.88.2.e14.

[7] H. Sies, Findings in redox biology: from H2O2 to oxidative stress, J. Biol. Chem. 295 (39) (Sep. 2020) 13458–13473, https://doi.org/10.1074/jbc.X120.015651.

[8] C. Henríquez-Olguin, et al., Cytosolic ROS production by NADPH oxidase 2 regulates muscle glucose uptake during exercise, Nat. Commun. 10 (1) (Oct. 2019), 4623, https://doi.org/10.1038/s41467-019-12523-9.

[9] E.L. Ostrom, A.P. Valencia, D.J. Marcinek, T. Traustadóttir, High intensity muscle stimulation activates a systemic Nrf2-mediated redox stress response, Free Radic. Biol. Med. 172 (Aug. 2021) 82–89, https://doi.org/10.1016/j.freeradbiomed.2021.05.039.

[10] A.J. Done, M.J. Gage, N.C. Nieto, T. Traustadóttir, Exercise-induced Nrf2-signaling is impaired in aging, Free Radic. Biol. Med. 96 (Jul. 2016) 130–138, https://doi.org/10.1016/j.freeradbiomed.2016.04.024.

[11] M.J. Jackson, A. Vasilaki, A. McArdle, Cellular mechanisms underlying oxidative stress in human exercise, Free Radic. Biol. Med. 98 (Sep. 2016) 13–17, https://doi.org/10.1016/j.freeradbiomed.2016.02.023.

[12] L.M. Popovic, et al., The effect of exhaustive exercise on oxidative stress generation and antioxidant defense in Guinea pigs, Adv. Clin. Exp. Med. Off. Organ Wroclaw Med. Univ. 21 (3) (2012) 313–320.

[13] X. Zhang, et al., Anti-fatigue effect of anwulignan *via* the NRF2 and PGC-1α signaling pathway in mice, Food Funct. 10 (12) (2019) 7755–7766, https://doi.org/10.1039/C9FO01182J.

[14] L. Li, H. Dong, E. Song, X. Xu, L. Liu, Y. Song, Nrf2/ARE pathway activation, HO-1 and NQO1 induction by polychlorinated biphenyl quinone is associated with reactive oxygen species and PI3K/AKT signaling, Chem. Biol. Interact. 209 (Feb. 2014) 56–67, https://doi.org/10.1016/j.cbi.2013.12.005.

[15] I. Dimauro, et al., Systemic response of antioxidants, heat shock proteins, and inflammatory biomarkers to short-lasting exercise training in healthy male subjects, Oxid. Med. Cell. Longev. (Nov. 2021) 1–15, https://doi.org/10.1155/2021/1938492, 2021.

[16] A. Vezzoli, L. Pugliese, M. Marzorati, F.R. Serpiello, A. La Torre, S. Porcelli, Time-course changes of oxidative stress response to high-intensity discontinuous training versus moderate-intensity continuous training in masters runners, PLoS One 9 (1) (Jan. 2014), e87506, https://doi.org/10.1371/journal.pone.0087506.

[17] A.L. Baggish, et al., Dynamic regulation of circulating microRNA during acute exhaustive exercise and sustained aerobic exercise training: circulating microRNA in exercise, J. Physiol. 589 (16) (Aug. 2011) 3983–3994, https://doi.org/10.1113/jphysiol.2011.213363.

[18] L.S. Chow, et al., Exerkines in health, resilience and disease, Nat. Rev. Endocrinol. 18 (5) (May 2022) 273–289, https://doi.org/10.1038/s41574-022-00641-2.

[19] A. Mendez-Gutierrez, et al., Exercise-induced changes on exerkines that might influence brown adipose tissue metabolism in young sedentary adults, Eur. J. Sport Sci. 23 (4) (Apr. 2023) 625–636, https://doi.org/10.1080/17461391.2022.2040597.

[20] C. Frühbeis, S. Helmig, S. Tug, P. Simon, E.-M. Krämer-Albers, Physical exercise induces rapid release of small extracellular vesicles into the circulation, J. Extracell. Vesicles 4 (1) (Jan. 2015), 28239, https://doi.org/10.3402/jev.v4.28239.

[21] M. Whitham, et al., Extracellular vesicles provide a means for tissue crosstalk during exercise, Cell Metabol. 27 (1) (Jan. 2018) 237–251, https://doi.org/10.1016/j.cmet.2017.12.001, e4.

[22] S. Bernardi, C. Balbi, Extracellular vesicles: from biomarkers to therapeutic tools, Biology 9 (9) (Aug. 2020) 258, https://doi.org/10.3390/biology9090258.

[23] J. Dong, B. Wu, W. Tian, Human adipose tissue-derived small extracellular vesicles promote soft tissue repair through modulating M1-to-M2 polarization of macrophages, Stem Cell Res. Ther. 14 (1) (Apr. 2023) 67, https://doi.org/10.1186/s13287-023-03306-7.

[24] G. Raposo, P.D. Stahl, Extracellular vesicles: a new communication paradigm? Nat. Rev. Mol. Cell Biol. 20 (9) (Sep. 2019) 509–510, https://doi.org/10.1038/s41580-019-0158-7.

[25] B. Estébanez, D. Jiménez-Pavón, C. Huang, M.J. Cuevas, J. González-Gallego, Effects of exercise on exosome release and cargo in in vivo and ex vivo models: a systematic review, J. Cell. Physiol. 236 (5) (May 2021) 3336–3353, https://doi.org/10.1002/jcp.30094.

[26] C. Tripisciano, R. Weiss, S. Karuthedom George, M.B. Fischer, V. Weber, Extracellular vesicles derived from platelets, red blood cells, and monocyte-like cells differ regarding their ability to induce factor XII-dependent thrombin generation, Front. Cell Dev. Biol. 8 (May 2020) 298, https://doi.org/10.3389/fcell.2020.00298.

[27] C. Tian, L. Gao, M.C. Zimmerman, I.H. Zucker, Myocardial infarction-induced microRNA-enriched exosomes contribute to cardiac Nrf2 dysregulation in chronic heart failure, Am. J. Physiol. Heart Circ. Physiol. 314 (5) (May 2018) H928–H939, https://doi.org/10.1152/ajpheart.00602.2017.

[28] F. Sabatier, et al., Type 1 and type 2 diabetic patients display different patterns of cellular microparticles, Diabetes 51 (9) (Sep. 2002) 2840–2845, https://doi.org/10.2337/diabetes.51.9.2840.

[29] S. Maggio, et al., Modulation of the circulating extracellular vesicles in response to different exercise regimens and study of their inflammatory effects, Int. J. Mol. Sci. 24 (3) (Feb. 2023), 3039, https://doi.org/10.3390/ijms24033039.

[30] M. Schild, et al., Effects of acute endurance exercise on plasma protein profiles of endurance-trained and untrained individuals over time, Mediat. Inflamm. (2016) 1–11, https://doi.org/10.1155/2016/4851935, 2016.

[31] A. Brahmer, et al., Platelets, endothelial cells and leukocytes contribute to the exercise-triggered release of extracellular vesicles into the circulation, J. Extracell. Vesicles 8 (1) (Dec. 2019), 1615820, https://doi.org/10.1080/20013078.2019.1615820.

[32] Z. Hou, et al., Longterm exercise-derived exosomal miR-342-5p: a novel exerkine for cardioprotection, Circ. Res. 124 (9) (Apr. 2019) 1386–1400, https://doi.org/10.1161/CIRCRESAHA.118.314635.

[33] X. Yin, et al., Time-course responses of muscle-specific MicroRNAs following acute uphill or downhill exercise in sprague-dawley rats, Front. Physiol. 10 (Oct. 2019), 1275, https://doi.org/10.3389/fphys.2019.01275.

[34] M. Guescini, et al., Muscle releases alpha-sarcoglycan positive extracellular vesicles carrying miRNAs in the bloodstream, PLoS One 10 (5) (May 2015), e0125094, https://doi.org/10.1371/journal.pone.0125094.

[35] Y. Bei, et al., Exercise-induced circulating extracellular vesicles protect against cardiac ischemia–reperfusion injury, Basic Res. Cardiol. 112 (4) (Jul. 2017) 38, https://doi.org/10.1007/s00395-017-0628-z.

[36] C. Ma, et al., Moderate exercise enhances endothelial progenitor cell exosomes release and function, Med. Sci. Sports Exerc. 50 (10) (Oct. 2018) 2024–2032, https://doi.org/10.1249/MSS.0000000000001672.

[37] J. Just, et al., Blood flow-restricted resistance exercise alters the surface profile, miRNA cargo and functional impact of circulating extracellular vesicles, Sci. Rep. 10 (1) (Apr. 2020), 5835, https://doi.org/10.1038/s41598-020-62456-3.

[38] M.L. Pollock, C. Foster, D. Schmidt, C. Hellman, A.C. Linnerud, A. Ward, Comparative analysis of physiologic responses to three different maximal graded exercise test protocols in healthy women, Am. Heart J. 103 (3) (Mar. 1982) 363–373, https://doi.org/10.1016/0002-8703(82)90275-7.

[39] J.A. Baecke, J. Burema, J.E. Frijters, A short questionnaire for the measurement of habitual physical activity in epidemiological studies, Am. J. Clin. Nutr. 36 (5) (Nov. 1982) 936–942, https://doi.org/10.1093/ajcn/36.5.936.

[40] G. Borg, Psychophysical scaling with applications in physical work and the perception of exertion, Scand. J. Work. Environ. Health 16 (1990) 55–58, https://doi.org/10.5271/sjweh.1815.

[41] S. Picciolini, et al., Detection and characterization of different brain-derived subpopulations of plasma exosomes by surface Plasmon resonance imaging, Anal. Chem. 90 (15) (Aug. 2018) 8873–8880, https://doi.org/10.1021/acs.analchem.8b00941.

[42] S. Picciolini, et al., An SPRi-based biosensor pilot study: analysis of multiple circulating extracellular vesicles and hippocampal volume in Alzheimer's disease, J. Pharm. Biomed. Anal. 192 (Jan. 2021), 113649, https://doi.org/10.1016/j.jpba.2020.113649.

[43] J. Rappsilber, M. Mann, Y. Ishihama, Protocol for micro-purification, enrichment, pre-fractionation and storage of peptides for proteomics using StageTips, Nat. Protoc. 2 (8) (Aug. 2007) 1896–1906, https://doi.org/10.1038/nprot.2007.261.

[44] J. Cox, N. Neuhauser, A. Michalski, R.A. Scheltema, J.V. Olsen, M. Mann, Andromeda: a peptide search engine integrated into the MaxQuant environment, J. Proteome Res. 10 (4) (Apr. 2011) 1794–1805, https://doi.org/10.1021/pr101065j.

[45] J. Cox, M.Y. Hein, C.A. Luber, I. Paron, N. Nagaraj, M. Mann, Accurate proteome-wide label-free quantification by delayed normalization and maximal peptide ratio extraction, termed MaxLFQ, Mol. Cell. Proteomics 13 (9) (Sep. 2014) 2513–2526, https://doi.org/10.1074/mcp.M113.031591.

[46] S. Tyanova, et al., The Perseus computational platform for comprehensive analysis of (prote)omics data, Nat. Methods 13 (9) (Sep. 2016) 731–740, https://doi.org/10.1038/nmeth.3901.

[47] E. Pianezzi, et al., Role of somatic cell sources in the maturation degree of human induced pluripotent stem cell-derived cardiomyocytes, Biochim. Biophys. Acta BBA - Mol. Cell Res. (3) (Mar. 2020), 118538, https://doi.org/10.1016/j.bbamcr.2019.118538, 1867.

[48] M.M. Bradford, A rapid and sensitive method for the quantitation of microgram quantities of protein utilizing the principle of protein-dye binding, Anal. Biochem. 72 (1–2) (May 1976) 248–254, https://doi.org/10.1016/0003-2697(76)90527-3.

[49] J.W. Irwin, N. Hedges, Measuring lipid oxidation, in: Understanding and Measuring the Shelf-Life of Food, Elsevier, 2004, pp. 289–316, https://doi.org/10.1533/9781855739024.2.289.

[50] E. Cappelli, et al., The passage from bone marrow niche to bloodstream triggers the metabolic impairment in Fanconi Anemia mononuclear cells, Redox Biol. 36 (Sep. 2020), 101618, https://doi.org/10.1016/j.redox.2020.101618.

[51] N. Bertola, P. Degan, E. Cappelli, S. Ravera, Mutated FANCA gene role in the modulation of energy metabolism and mitochondrial dynamics in head and neck squamous cell carcinoma, Cells 11 (15) (Jul. 2022), 2353, https://doi.org/10.3390/cells11152353.

[52] S. Ravera, et al., 808-nm photobiomodulation affects the viability of a head and neck squamous carcinoma cellular model, acting on energy metabolism and oxidative stress production, Biomedicines 9 (11) (Nov. 2021) 1717, https://doi.org/10.3390/biomedicines9111717.

[53] J. Zielonka, J. Vasquez-Vivar, B. Kalyanaraman, Detection of 2-hydroxyethidium in cellular systems: a unique marker product of superoxide and hydroethidine, Nat. Protoc. 3 (1) (Jan. 2008), https://doi.org/10.1038/nprot.2007.473. Art. no. 1.

[54] G.F. Fletcher, et al., Exercise standards for testing and training: a scientific statement from the American heart association, Circulation 128 (8) (Aug. 2013) 873–934, https://doi.org/10.1161/CIR.0b013e31829b5b44.

[55] C. Théry, et al., Minimal information for studies of extracellular vesicles 2018 (MISEV2018): a position statement of the International Society for Extracellular Vesicles and update of the MISEV2014 guidelines, J. Extracell. Vesicles 7 (1) (Dec. 2018), 1535750, https://doi.org/10.1080/20013078.2018.1535750.

[56] P. Cizmar, Y. Yuana, Detection and characterization of extracellular vesicles by transmission and cryo-transmission Electron microscopy, in: W.P. Kuo, S. Jia (Eds.), Extracellular Vesicles, Methods in Molecular Biology, vol. 1660, Springer New York, New York, NY, 2017, pp. 221–232, https://doi.org/10.1007/978-1-4939-7253-1_18.

[57] N. Comfort, et al., Isolation and characterization of extracellular vesicles in saliva of children with asthma, Extracell. Vesicles Circ. Nucleic Acids (2021), https://doi.org/10.20517/evcna.2020.09.

[58] Z. Zhao, H. Wijerathne, A.K. Godwin, S.A. Soper, Isolation and analysis methods of extracellular vesicles (EVs), Extracell. Vesicles Circ. Nucleic Acids (2021), https://doi.org/10.20517/evcna.2021.07.

[59] N. Karimi, et al., Detailed analysis of the plasma extracellular vesicle proteome after separation from lipoproteins, Cell. Mol. Life Sci. 75 (15) (Aug. 2018) 2873–2886, https://doi.org/10.1007/s00018-018-2773-4.

[60] C. Tallon, et al., Inhibition of neutral sphingomyelinase 2 reduces extracellular vesicle release from neurons, oligodendrocytes, and activated microglial cells following acute brain injury, Biochem. Pharmacol. 194 (Dec. 2021), 114796, https://doi.org/10.1016/j.bcp.2021.114796.

[61] J. Zhang, et al., ROS and ROS-mediated cellular signaling, Oxid. Med. Cell. Longev. (2016) 1–18, https://doi.org/10.1155/2016/4350965, 2016.

[62] C. Gaucher, A. Boudier, J. Bonetti, I. Clarot, P. Leroy, M. Parent, Glutathione: antioxidant properties dedicated to nanotechnologies, Antioxidants 7 (5) (Apr. 2018) 62, https://doi.org/10.3390/antiox7050062.

[63] C. Berzosa, et al., Acute exercise increases plasma total antioxidant status and antioxidant enzyme activities in untrained men, J. Biomed. Biotechnol. (2011) 1–7, https://doi.org/10.1155/2011/540458, 2011.

[64] P. Wang, C.G. Li, Z. Qi, D. Cui, S. Ding, Acute exercise induced mitochondrial H_2O_2 production in mouse skeletal muscle: association with p^{66Shc} and FOXO3a signaling and antioxidant enzymes, Oxid. Med. Cell. Longev. (2015) 1–10, https://doi.org/10.1155/2015/536456, 2015.

[65] E. García-Domínguez, et al., Glucose 6-P dehydrogenase—an antioxidant enzyme with regulatory functions in skeletal muscle during exercise, Cells 11 (19) (Sep. 2022), 3041, https://doi.org/10.3390/cells11193041.

[66] H. Jing, G. Zou, F. Hao, H. Wang, S. Wang, Hsp27 reduces cold ischemia-reperfusion injury in heart transplantation through regulation of NF-κB and PUMA signaling, Int. J. Clin. Exp. Pathol. 11 (1) (2018) 281–292.

[67] A. Vidyasagar, N.A. Wilson, A. Djamali, Heat shock protein 27 (HSP27): biomarker of disease and therapeutic target, Fibrogenesis Tissue Repair 5 (1) (Dec. 2012) 7, https://doi.org/10.1186/1755-1536-5-7.

[68] J.M. Vicencio, et al., Plasma exosomes protect the myocardium from ischemia-reperfusion injury, J. Am. Coll. Cardiol. 65 (15) (Apr. 2015) 1525–1536, https://doi.org/10.1016/j.jacc.2015.02.026.

[69] M. Barzegar, et al., Human placental mesenchymal stem cells improve stroke outcomes via extracellular vesicles-mediated preservation of cerebral blood flow, EBioMedicine 63 (Jan. 2021), 103161, https://doi.org/10.1016/j.ebiom.2020.103161.

[70] G. Milano, et al., Intravenous administration of cardiac progenitor cell-derived exosomes protects against doxorubicin/trastuzumab-induced cardiac toxicity, Cardiovasc. Res. (Apr. 2019), cvz108, https://doi.org/10.1093/cvr/cvz108.

[71] Y. Kobayashi, et al., Protein composition of circulating extracellular vesicles immediately changed by particular short time of high-intensity interval training exercise, Front. Physiol. 12 (Jul. 2021), 693007, https://doi.org/10.3389/fphys.2021.693007.

[72] A.E. Rigamonti, et al., Effects of an acute bout of exercise on circulating extracellular vesicles: tissue-, sex-, and BMI-related differences, Int. J. Obes. 44 (5) (May 2020) 1108–1118, https://doi.org/10.1038/s41366-019-0460-7.

[73] S. Atienzar-Aroca, et al., Oxidative stress in retinal pigment epithelium cells increases exosome secretion and promotes angiogenesis in endothelial cells, J. Cell Mol. Med. 20 (8) (Aug. 2016) 1457–1466, https://doi.org/10.1111/jcmm.12834.

[74] S. Atienzar-Aroca, et al., Role of retinal pigment epithelium-derived exosomes and autophagy in new blood vessel formation, J. Cell Mol. Med. 22 (11) (Nov. 2018) 5244–5256, https://doi.org/10.1111/jcmm.13730.

[75] Y. Zhang, et al., Exercise and metformin intervention prevents lipotoxicity-induced hepatocyte apoptosis by alleviating oxidative and ER stress and activating the AMPK/Nrf2/HO-1 signaling pathway in db/db mice, Oxid. Med. Cell. Longev. (Sep. 2022) 1–13, https://doi.org/10.1155/2022/2297268, 2022.

[76] M. Bouzid, E. Filaire, R. Matran, S. Robin, C. Fabre, Lifelong voluntary exercise modulates age-related changes in oxidative stress, Int. J. Sports Med. 39 (1) (Jan. 2018) 21–28, https://doi.org/10.1055/s-0043-119882.

[77] C. Simioni, et al., Oxidative stress: role of physical exercise and antioxidant nutraceuticals in adulthood and aging, Oncotarget 9 (24) (Mar. 2018) 17181–17198, https://doi.org/10.18632/oncotarget.24729.

[78] R. Furrer, P.S. Eisele, A. Schmidt, M. Beer, C. Handschin, Paracrine cross-talk between skeletal muscle and macrophages in exercise by PGC-1α-controlled BNP, Sci. Rep. 7 (1) (Jan. 2017), 40789, https://doi.org/10.1038/srep40789.

[79] M.E. Davis, H. Cai, L. McCann, T. Fukai, D.G. Harrison, Role of c-Src in regulation of endothelial nitric oxide synthase expression during exercise training, Am. J. Physiol. Heart Circ. Physiol. 284 (4) (Apr. 2003) H1449–H1453, https://doi.org/10.1152/ajpheart.00918.2002.

[80] M.M. Cortese-Krott, et al., Red blood cell eNOS is cardioprotective in acute myocardial infarction, Redox Biol. 54 (Aug. 2022), 102370, https://doi.org/10.1016/j.redox.2022.102370.

[81] S.M. Davidson, J.A. Riquelme, Y. Zheng, J.M. Vicencio, S. Lavandero, D.M. Yellon, Endothelial cells release cardioprotective exosomes that may contribute to ischaemic preconditioning, Sci. Rep. 8 (1) (Oct. 2018), 15885, https://doi.org/10.1038/s41598-018-34357-z.

[82] F. Ravera, et al., Endothelial cell-derived extracellular vesicles exert cardio-protective effect via their protein cargo, Eur. Heart J. 41 (2) (Nov. 2020), https://doi.org/10.1093/ehjci/ehaa946.3767 ehaa946.3767.

[83] A. Alberro, L. Iparraguirre, A. Fernandes, D. Otaegui, Extracellular vesicles in blood: sources, effects, and applications, Int. J. Mol. Sci. 22 (15) (Jul. 2021), 8163, https://doi.org/10.3390/ijms22158163.

[84] S.E. Headland, H.R. Jones, A.S.V. D'Sa, M. Perretti, L.V. Norling, Cutting-edge analysis of extracellular microparticles using ImageStreamX imaging flow cytometry, Sci. Rep. 4 (1) (Jun. 2014), 5237, https://doi.org/10.1038/srep05237.

[85] Y. Li, et al., EV-origin: enumerating the tissue-cellular origin of circulating extracellular vesicles using exLR profile, Comput. Struct. Biotechnol. J. 18 (2020) 2851–2859, https://doi.org/10.1016/j.csbj.2020.10.002.

[86] K. Thangaraju, S.N. Neerukonda, U. Katneni, P.W. Buehler, Extracellular vesicles from red blood cells and their evolving roles in health, coagulopathy and therapy, Int. J. Mol. Sci. 22 (1) (Dec. 2020) 153, https://doi.org/10.3390/ijms22010153.

[87] M.P. Murphy, et al., Guidelines for measuring reactive oxygen species and oxidative damage in cells and in vivo, Nat. Metab. 4 (6) (Jun. 2022), https://doi.org/10.1038/s42255-022-00591-z, 6.

[88] F. He, X. Ru, T. Wen, NRF2, a transcription factor for stress response and beyond, Int. J. Mol. Sci. 21 (13) (Jul. 2020), 4777, https://doi.org/10.3390/ijms21134777.

[89] X. Li, et al., Exosomes from adipose-derived stem cells overexpressing Nrf2 accelerate cutaneous wound healing by promoting vascularization in a diabetic foot ulcer rat model, Exp. Mol. Med. 50 (4) (Apr. 2018) 1–14, https://doi.org/10.1038/s12276-018-0058-5.

[90] M. Ge, et al., Brg1-mediated Nrf2/HO-1 pathway activation alleviates hepatic ischemia–reperfusion injury, Cell Death Dis. 8 (6) (Jun. 2017), https://doi.org/10.1038/cddis.2017.236 e2841–e2841.

[91] J.A. Fafián-Labora, J.A. Rodríguez-Navarro, A. O'Loghlen, Small extracellular vesicles have GST activity and ameliorate senescence-related tissue damage, Cell Metabol. 32 (1) (Jul. 2020) 71–86, https://doi.org/10.1016/j.cmet.2020.06.004, e5.

[92] C. Mas-Bargues, J. Sanz-Ros, N. Romero-García, J. Huete-Acevedo, M. Dromant, C. Borrás, Small extracellular vesicles from senescent stem cells trigger adaptive mechanisms in young stem cells by increasing antioxidant enzyme expression, Redox Biol. 62 (Jun. 2023), 102668, https://doi.org/10.1016/j.redox.2023.102668.